The molybdenum isotope composition of modern and ancient stromatolites

Marie Thoby

université de bretagne occidentale

MASTER SML
SCIENCES DE LA MER ET DU LITTORAL

expérience MENTION
Géosciences
SPÉCIALITÉ
Terre Externe

THOBY Marie

La composition isotopique du molybdène des stromatolites modernes et anciens

Mémoire de stage de Master 2
Année Universitaire **2014-2015**
Structure d'accueil : **Laboratoire Domaine Océanique**
Tuteur universitaire : **GRAINDORGE David**
Maître de stage : **LALONDE Stefan**

UBO CNRS IRD iuem INSTITUT UNIVERSITAIRE EUROPÉEN DE LA MER

UNIVERSITY OF ALBERTA

IUEM-OSU DOMAINES OCEANIQUES CNRS-UBO

Thoby Marie

The molybdenum isotope composition of modern and ancient stromatolites

Supervisor: LALONDE Stefan

University Supervisor: GRAINDORGE David

Master 2 2014-2015

université de bretagne occidentale

L'Université est une chance

ENGAGEMENT DE NON PLAGIAT

Je soussigné-e Marie Thoby

assure avoir pris connaissance de la charte anti plagiat de l'université de Bretagne occidentale.

Je déclare être pleinement conscient-e que le plagiat total ou partiel de documents publiés sous différentes formes, y compris sur internet, constitue une violation des droits d'auteur ainsi qu'une fraude caractérisée.

Je m'engage à citer toutes les sources que j'ai utilisées pour rédiger ce travail.

Signature

Document à insérer en première page de tous les rapports, dossiers et mémoires.

The primitive Earth was characterized by an oxygen-poor ocean–atmosphere system, and experienced a significant increase in oxygen concentrations during the Great Oxidation Event (GOE) ca 2.45 Ga. This event is generally believed to be linked in some way to oxygenic photosynthesis by bacteria. However, it is becoming commonly accepted that “whiffs” of oxygen existed before the GOE. To shed new light on this emerging paradigm, here we present molybdenum (Mo) isotopic data for modern stromatolites from Bacalar lagoon, Mexico, and ancient stromatolites from Archean sediments deposited ca. 2.52 Ga (Ghaap Group, South Africa), 2.8 Ga (Steep Rock, Canada), and 2.96 Ga (Red Lake, Canada). Modern samples record a molybdenum isotopic signature that appears related to the water from which they grew, supporting the idea that the molybdenum isotopic composition of carbonates is a robust proxy for examining paleo-redox conditions of environments where carbonates were precipitated. Ancient stromatolites reveal evidence for oxygen in the environment at 2.96 Ga at 2.8 Ga, while stromatolites from the Ghaap Group (2.52 Ga) appear to have grown under poorly-oxygenated conditions. My data suggests that oxygenic photosynthesis existed yet at least 0.61 Ga before the rise of atmospheric oxygen. Moreover, the consistent signal for oxygen in the environment at this time could be indicative of a constant period of mild oxygenation, rather than local oases as previously proposed.

La Terre Primitive se distingue par l’absence d’oxygène dans l’atmosphère et les océans. La croissance de la concentration en oxygène de l’atmosphère fut déterminée par le Grand Évènement d’Oxydation (GEO) aux alentours de 2.45 Ga et aurait été influencée par l’augmentation de l’utilisation de la photosynthèse oxygénique par les formes de vies primitives que sont les bactéries. De plus, il est reconnu que des pulses d’oxygène ont existé avant le GOE. Nous présentons ici des données d’isotopie du molybdène de stromatolites modernes provenant du lagon du Bacalar au Mexique et de stromatolites anciens issus de formations archéennes à 2.52 Ga (Groupe Ghaap, Afrique du Sud), à 2.8 Ga (Steep Rock, Canada) et à 2.96 Ga (Red Lake, Canada). Les échantillons modernes montrent une signature isotopique du molybdène de l’eau dans laquelle ils ont été formés. Cela justifie l’utilisation de la composition isotopique en molybdène des carbonates pour connaître les conditions redox de l’environnement marin dans lequel ils ont précipité. Les stromatolites anciens indiquent la présence d’environnements oxygénés dès 2.96 Ga et à 2.8 Ga tandis que les échantillons du Groupe Ghaap (2.52 Ga) se sont formés en condition anoxique. Nous pensons que la photosynthèse oxygénique existait déjà il y a plus de 0.61 Ga avant le GOE et que ces environnements oxygénés pourraient correspondre à de longue période oxygénées plutôt qu’aux oasis locaux suggérés précédemment.

Remerciements :

Je tiens à remercier chaleureusement Stefan Lalonde, qui m'a vu un jour débarquer dans son bureau avec une idée précise en tête et qui m'a permis de la réaliser. Sa passion et son enthousiasme si contagieux rendent l'échange et le travail captivant. Son perfectionnisme et son besoin de faire les choses à la dernière minute ne font peut être pas partie de mes facultés mais je compte bien y remédier dans les années à venir au cours de la thèse. Merci beaucoup Stefan de croire en mes capacités scientifiques.

Merci aussi à Kurt Konhauser pour son soutient pour ce projet à court et à long terme en m'offrant la possibilité de continuer en thèse. Merci aussi pour ses échantillons de stomatolite.

Merci à Olivier Rouxel qui m'a laisser utiliser ses standards, ses doubles-spikes et ses solutions pour toute ma chimie.

Un Merci particulier à Manu pour ses conseils, sa passion pour la recherche analytique et pour avoir bravé l'Apex défaillant et le 1er mai afin d'avoir des résultats pour ce stage !

Merci à Dawn Sumner et Philip Fralick pour m'avoir permis de travailler sur leurs échantillons de stromatolites anciens et à Pierre SansJofre pour les carbonates sur lesquels j'ai pu effectuer le développement analytique.

Merci à Clair, Marie Laure, Céline et Yohann pour leurs accueils et leurs patiences face à mes petites boulettes de carbonate et mes éruptions d'échantillons !

Merci à toute l'équipe du LDO pour l'accueil au sein du laboratoire, pour croire en ce projet et pour le soutient reçu dans notre « combat » de petit stagiaire.

Merci à toute l'équipe du LDO pour l'accueil au sein du laboratoire, pour croire en ce projet et pour le soutient reçu dans notre « combat » de petit stagiaire.

Merci à mes collègues de salle blanche, Maxence et Arthur, avec leur bonne humeur, imitation du Jurassique et les concerts ! Un merci particulier à Maxence pour m'avoir aidé dans la chimie et dans la préparation des analyses.

Merci à Virgil pour son soutient, ses coups de main, ses coups de gueule et toutes les discussion autour de cette passion qu'est la science!

Merci à Tyler pour sa bonne humeur, les corrections d'anglais qu'il a apporté à ce rapport et son enseignement sur la rédaction d'article en anglais. On se revoie, je l'espère, bientôt au Canada !

Merci à mon collègue de bureau Mr Steven, sans qui je me serai pris la tête beaucoup plus souvent. Longue vie aux craquages et aux hymnes Celtes !

Merci à Kroll sans qui les choses ne tourneraient pas rond ! Tu gères la fougère, on t'aime tous !

Merci Dominique pour te démener dans la recherche d'articles introuvables ! Je ne sais pas comment vont faire les prochaines promos !

Merci à ma famille pour m'avoir accueilli afin que je rédige les pieds dans l'eau face à la petite mer et à l'île Tristan.
Merci à Guillaume qui un soir de long week-end ma vu se réfugier chez lui pour pouvoir avance l'écriture dans le calme !
Merci aux amis qui mon sortie l'esprit que ce moment de rédaction se face avec plaisir entre des moments de natation, des week-end de sauvage à la sauvage et la construction de bateau en carton. Ca va cartonner ce week-end Jean-Mi ! A l'abordage !
Merci à toute la promo avec qui j'ai passé d'excellents moments au long de ces deux années et vécu des choses inoubliable tel le séisme de minuit dans une salle de court, un voyage formidable en Italie, des conneries, des craquages, des passions. Alors tous à vos fossiles et bon vent !

En avant la Science !

Table of Contents

INTRODUCTION **4**

1. GENERAL CONTEXT **6**

1.1 THE EARLIEST LIFE ON EARTH 6

1.2 FROM PHOTOSYNTHETIC BACTERIA TO STROMATOLITES 9

1.3 MOLYBDENUM AS A REDOX PROXY 10

1.3.1 Molybdenum geochemistry *10*

1.3.2 Molybdenum isotopes *11*

2. MATERIALS AND METHODS **16**

2.1. MATERIALS 16

2.2. PRINCIPLES OF MO ISOTOPE MEASUREMENT 17

2.2.1. MC-ICP-MS *17*

2.2.2. Sample preparation *17*

2.2.3. The isotope double spike method *18*

2.3. METHODS OF THIS STUDY 18

2.4. MO ISOTOPIC MEASUREMENTS 21

3. RESULTS **23**

4. DISCUSSION **29**

4.1. MODERN STROMATOLITES 29

4.2. 2.52 GA STROMATOLITES, GAMOHAAN FORMATION, SOUTH AFRICA 30

4.3. 2.8 GA STROMATOLITES, STEEP ROCK, CANADA 31

4.4. 2.96 GA STROMATOLITES, RED LAKE, CANADA 31

4.5. EVIDENCE FOR OXYGEN AND OXYGENIC PHOTOSYNTHESIS BEFORE THE GOE 32

CONCLUSION **34**

BIBLIOGRAPHY **35**

ANNEXES **38**

Tables and Figures

Figure 1: Evolution of Earth's atmospheric oxygen content through geological time. Purple and blue shaded zones represent classic and emerging views, respectively. Arrows represent possible 'whiffs' of O2 before the Great Oxidation Event (GOE) ca. 2.45 Ga. From Lyons et al. (2014). *5*

Figure 2.1 : Carbon isotope signatures in a) Pilbara sediments (>3.250 Ga, West Australia); b) Isua BIF (~3.8 Ga, West Greenland) and c) BIF on Akilia island (>3.85 Ga, West Greenland). Characteristic ranges of δ13C in organic and inorganic matter are presented in d. From Mojzsis et al. (1996). *6*

Figure 2.2: Earth's earliest fossil records: a) Microfossils; Examples of hollow, tubular, sheath-like microfossil Strelley Pool Chert, Warrawoona Group, Western Australia (3.45 Ga; from Wacey et al., 2011), and b) Oldest known stromatolite occurrence, also in the Strelley Pool Chert, Warrawoona Group, Western Australia (photo courtesy S. Lalonde). *7*

Figure 2.3: Geobiological clock from Konhauser (2007), adapted from Des Marais (2000). *7*

Figure 2.4: Schematic of carbonate biomineralization by cyanobacteria. From Konhauser (2007), adapted from Thompson and Ferris (1990). *9*

Figure 2.5: Compilation of Mo isotopic signature of Mo sources of seawater. The mean of modern seawater and crust Mo isotopic signature are represented by respectively a dash line and a full line. *14*

Figure 2.6: Compilation of Mo isotopic signature of Mo sinks of seawater. The mean of modern and Proterozoic seawater and crust Mo isotopic signature are represented by respectively two dash lines and a full line. *15*

Figure 3.1: Measurement of Mo concentration by double spike isotope dilution using the MC-ICP-MS Neptune. Red columns: measurement after a total attack with 6N HCl according to the protocol of Voegelin et al. (2009). Blue columns: measurement after a weak leach by 5% acetic acid according Rongemaille et al. (2011). *19*

Figure 3.2: Elution of molybdenum from SDO-1, SPEX, and SPEX-CAMIL32 column tests. Measurements were performed by HR-ICP-MS. *20*

Figure 3.3: Mo yields through both chromatographic columns used to concentrate and purify molybdenum. *21*

Figure 3.4: Elution of major elements in the SDO-1 and Camil elution tests. Measurements were performed by ICP-AES. *21*

Figure 4.1: Correlation between δ95/98Mo and δ97/ 98Mo with a slope equal to the relative mass differences of 97Mo/98Mo (1) and 95Mo/98Mo (3) support an isobaric interference-free measurement of all these isotopes. *23*

Table 1: Results of Mo isotopic analyses of modern and ancient stromatolites. δ^{98}MoSRM3134 values were obtained by the addition of 0.34‰ to the RochMo2–normalized values, as per Goldberg et al. (2013). *24*

Figure 4.2: δ^{98}Mo and Mo concentrations of modern stromatolites from Bacalar lagoon, Mexico. *25*

Figure 4.3: δ^{98}Mo and Mo concentrations of ancient stromatolites from the Gamohaan formation, South Africa, 2.52Ga. *25*

Figure 4.4: δ^{98}Mo and Mo concentrations of ancient stromatolites from Steep Rock, Canada, 2.8Ga. *26*

Figure 4.5: δ^{98}Mo and Mo concentrations of ancient stromatolites from Red Lake, Canada, 2.96Ga. *26*

Figure 4.6: $\delta^{98/95}$Mo values of modern and ancient stromatolites examined in this study. *28*

Figure 5.1: Mo isotopic compositions of Bacalar modern stromatolites from this study (blue points) appear to overlap with the modern river array (grey area; Archer and Vance, 2008). However, a mixing model based on the composition of continental crust (δ^{98}Mo=0‰, Siebert et al. (2003) and Mo=1100ppb; Rudnick and Gao (2003)) and

the isotopically heaviest stromatolite in this area (δ^{98}Mo =1.55‰ and Mo=6.15ppb) suggests a detrital dependence. 29

Figure 5.2: Selected Mo isotopic data throughout geological time. Mo isotopic compositions of the different types of rocks are from this study and as well as others (see legend). These results suggest a new emerging picture of redox evolution though geological time, with consistent Mo isotope evidence for at least transient oxygen in the environment at 2.96 Ga and 2.8 Ga. For comparison, data for modern carbonates and seawater are shown to present to represent the modern oxygenated environment. 32

Introduction

The concentration of oxygen in the oceans and atmosphere has evolved significantly over geological time (Holland, 2006). Multiple studies using various mineralogical observations (e.g., occurrence of detrital pyrite and iron formation; Rasmussen and Buick, 1999; Klein, 2005) and geochemical data (e.g., $\delta^{13}C$ and $\Delta^{33}S$; Karhu and Holland, 1996; Farquhar et al., 2000) have demonstrated that the quantity of oxygen in the atmosphere was 10^{-5} times lower than the present atmospheric level (PAL) prior to about 2.5 Ga (Figure 1; Holland, 2006; Lyons et al., 2014; Pavlov and Kasting, 2002). Nearly all of these studies have linked the rise of atmospheric oxygen to the evolution and activity of microbial life (Holland, 2006; Lyons et al., 2014). The first sustained increase in Earth's atmospheric oxygen occurred around 2.4 Ga and is commonly know as the Great Oxidation Event (GOE) (Bekker et al., 2004). While the GOE has traditionally been attributed to the development of oxygenic photosynthesis by cyanobacteria (e.g., Awramik, 1992; Lyons et al., 2014), the emerging picture is more nuanced. Recent studies have now shown that 1) local "oases" or "whiffs" of oxygen may have been present before the GOE (Figure 1; see Anbar et al., 2007; Crowe et al., 2013; Lalonde and Konhauser, 2015; Lyons et al., 2014; Planavsky et al., 2014), and 2) oxygenic photosynthesis may have existed as far back as 3.75 Ga (the oldest sedimentary record), well before the GOE. Rosing and Frei (2004) considered low $\delta^{13}C_{org}$ values in Earth's oldest sediments to be evidence of oxygenic photosynthesis at 3.75 Ga, whereas Awramik (1992) considered the earliest appearance of oxygenic photosynthesis to be associated with the oldest known stromatolite occurrence ca. 3.5 Ga. However, light carbon isotope enrichments and the occurrence of stromatolites may both be explained by non-oxygenic photosynthesis. Organic biomarkers have also been used to argue for oxygenic photosynthesis ca. 2.7 Ga (see review by Buick, 2008), but this data has since been refuted as resulting from later contamination (Rasmussen et al., 2008). In recent years, attention has turned to geochemical data (elemental and isotopic enrichments) of metals whose cycling appears highly sensitive to the presence of free O_2.

Planavsky et al. (2014) reported such evidence of oxygenic photosynthesis at 2.95 Ga by inspecting the correlation between molybdenum (Mo) isotopic signatures and the ratio of iron to manganese in deep-water sediments from the Pongola Supergroup, S. Africa. Molybdenum displays a characteristically light isotope signature when adsorbed to manganese oxides, which themselves require significant free O_2 to form. However, the strong fractionation associated with Mo adsorption to manganese oxides makes it difficult to extrapolate back to the Mo isotope composition of seawater due to potential Ryleigh distillation effects. In the case of partial absorption of molybdenum, its isotopic signature will be significantly lighter than seawater, whereas total

absorption would result in signatures closer to contemporaneous seawater. Recent work by Voegelin et al. (2009) has shown the molybdenum isotope composition of carbonates better represents the oceanic Mo reservoir without potential artefacts from partial absorption.

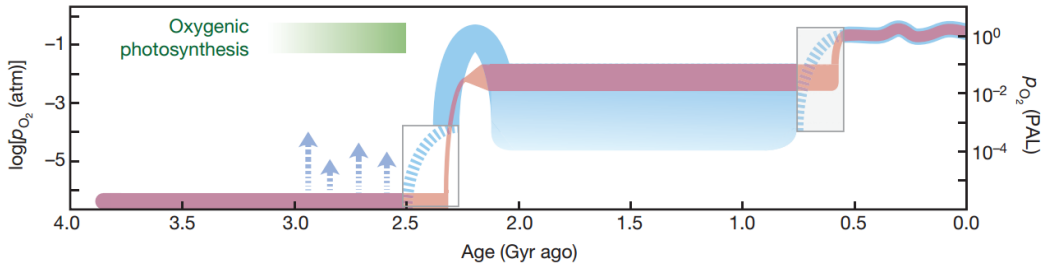

Figure 1: Evolution of Earth's atmospheric oxygen content through geological time. Purple and blue shaded zones represent classic and emerging views, respectively. Arrows represent possible 'whiffs' of O2 before the Great Oxidation Event (GOE) ca. 2.45 Ga. From Lyons et al. (2014).

The main goals of my MSc project were twofold: (1) to use the molybdenum isotope composition of Precambrian carbonates to shed new light on the origin of oxygenic photosynthesis, and (2) determine the phototrophic pathway used by bacteria in building oldest macrofossil records of Earth: stromatolites. Samples analysed in this study include ancient stromatolites from Red Lake, Canada (2.96 Ga), Steep Rock, Canada (2.8 Ga), the Gamohaan formation, South Africa (2.52 Ga), and modern freshwater stromatolites from Laguna Bacalar, Mexico.

This study was conducted under the supervision of Stefan Lalonde, CNRS researcher in the Laboratoire Domaines Océaniques (LDO). It could not have been completed without the assistance and co-funding of Professor Kurt Konhauser (University of Alberta), who also aided in the collection of stromatolites samples. Professors Philip Fralick (Lakehead University) and Dawn Sumner (University of California Davis) kindly provided Precambrian samples for this study. Molybdenum isotope analyses was performed at the Pôle Spectrométrie Océan (PSO) Brest with the assistance of IFREMER Research Scientist Olivier Rouxel. This work constitutes a preliminary study of the transition metal isotope compositions in modern and ancient stromatolites, which will be expanded upon during a subsequent PhD project.

1. General Context

1.1 The earliest life on Earth

The oldest potential records of life on Earth are isotopic signatures. Mojzsis et al. (1996) reported that the Banded Iron Formation (BIF) and chert from West Greenland (Akilia Island, ~3.85 Ga and Isua, ~3.8Ga) contain potentially biogenic light carbon isotopic signatures (Figure 2.1). Measurements were made on carbonaceous material inclusions in apatite minerals $Ca_5(PO_4)_3(OH,F)$. Phosphate is an essential element for life, and this diagenetic mineral may have crystallised from a P-rich biological source, as it often does today (Krajewshi et al., 2014). While metamorphism may have led to degassing of isotopically heavy C and enrichment of the residue in the light isotope, it remains difficult to explain the observed light C isotope composition of these rocks by metamorphism alone (Mojzsis et al., 1996).

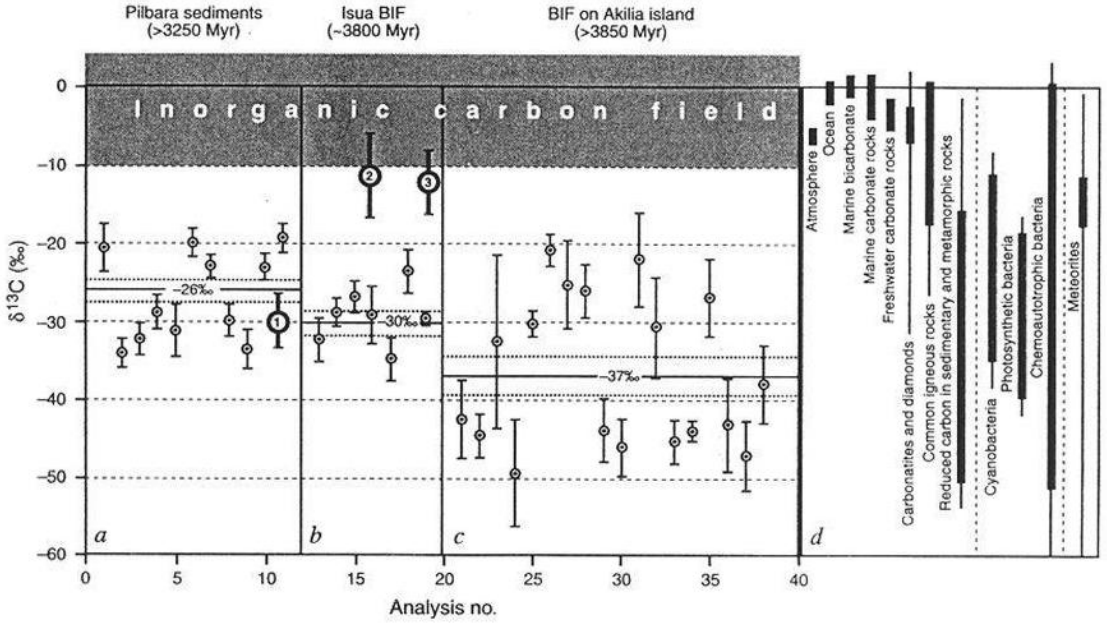

Figure 2.1 : Carbon isotope signatures in a) Pilbara sediments (>3.250 Ga, West Australia); b) Isua BIF (~3.8 Ga, West Greenland) and c) BIF on Akilia island (>3.85 Ga, West Greenland). Characteristic ranges of δ13C in organic and inorganic matter are presented in d. From Mojzsis et al. (1996).

This early isotopic record is reinforced by microfossil evidence discovered in the Swaziland Supergroup, South Africa (3.5 Ga; Walsh, 1992) and the Strelley Pool Chert, Western Australia (3.5 Ga; Wacey et al., 2011). Although they were formed very early in Earth's history, these complex microfossils (Figure 2.2a) were taken to reflect the proliferation of bacterial life to a relatively advanced stage by this time.

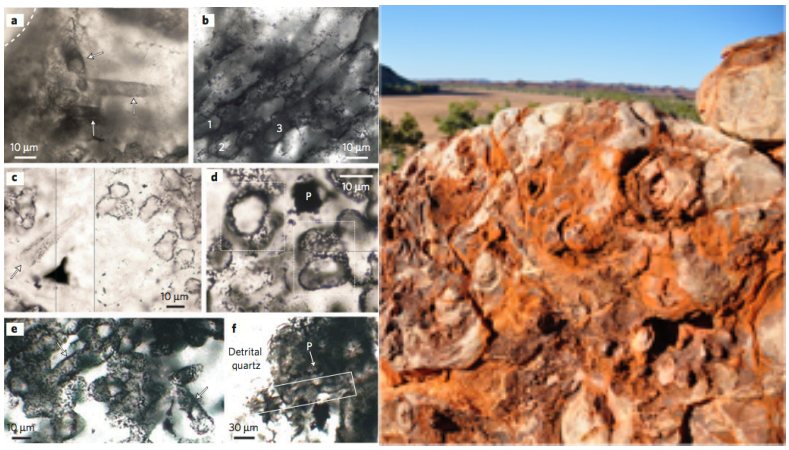

Figure 2.2: Earth's earliest fossil records: a) Microfossils; Examples of hollow, tubular, sheath-like microfossil Strelley Pool Chert, Warrawoona Group, Western Australia (3.45 Ga; from Wacey et al., 2011), and b) Oldest known stromatolite occurrence, also in the Strelley Pool Chert, Warrawoona Group, Western Australia (photo courtesy S. Lalonde).

Molecular phylogenetic data provides further information on life's first cells (for an overview see Konhauser, 2007). The first life forms were likely anaerobic chemolithoautotrophs (Figure 2.3); they depended on inorganic sources of essential elements for life (e.g., carbon, nitrogen) and their energy was produced by catalysis of redox reactions using inorganic compounds available in their environment. With the evolution of photosynthesis, bacteria gained independence from local reductants, sourcing their reducing power from sunlight instead.

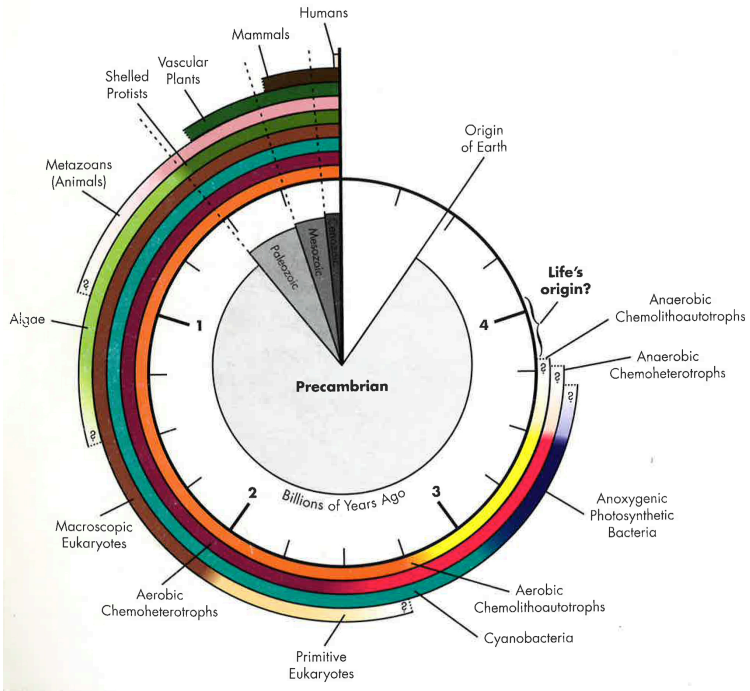

Figure 2.3: Geobiological clock from Konhauser (2007), adapted from Des Marais (2000).

Photosynthesis permits synthesis of organic matter using light from the sun as a source of reducing power. Sunlight is captured by light-harvesting pigments (chlorophyll, bacteriochlorophyll), and depending on the radiative environment (e.g. at the surface vs. at depth in a water column, under minerals or in a mat with other bacteria, or as a function of water opacity), different phototrophic bacteria with different types of pigments thrive on specific wavelengths of sunlight. The CO_2 used for the reaction can come from inorganic sources (photoautotrophy) or organic matter (photoheterotrophy). There two fundamental different kinds of photosynthesis: (i) anoxygenic photosynthesis (no O_2 production) and (ii) oxygenic photosynthesis (O_2-producing). The earliest phototrophic bacteria are thought to have grown in environments with abundant reductants, namely H_2S and Fe^{2+}. Phylogenetic data indicate that the earliest photosynthesizers were dependent on these sources of reducing power, and the process was anoxygenic. More specifically, anoxygenic photosynthesizers are divided into two groups based on their source of reducing power:

1) phototrophic sulfur oxidizers (green-sulfur or purple-sulfur bacteria) that use hydrogen sulphide (H_2S) or elemental sulfur (S^0) as their electron source (Kelly, 1974):

$$3H_2S + 6CO_2 + 6H_2O \rightarrow C_6H_{12}O_6 + 3SO_4^{2-} + 6H^+ \quad (1)$$

$$12S^0 + 18CO_2 + 30H_2O \rightarrow 3C_6H_{12}O_6 + 12SO_4^{2-} + 24H^+ \quad (2)$$

2) anoxygenic photoferrotrophs use Fe^{2+} as a reductant for the synthesis of organic matter. Photoferrotrophic bacteria generate large amounts of Fe(III) minerals as a waste product, a phenomena that has been implicated in the deposition of Precambrian BIF (Konhauser et al., 2002). Heising et al. (1999) defined the photoferrotrophic reaction as:

$$24Fe^{2+} + 6CO_2 + 66H_2O \rightarrow C_6H_{12}O_6 + 24Fe(OH)_3 + 48H^+ \quad (3)$$

Eventually, bacteria evolved the ability to oxidize water, giving rise to oxygenic photosynthesis. Performed by modern cyanobacteria and plants, this photosynthesic pathway produces free oxygen (O_2) according to the follow reaction:

$$6H_2O + 6CO_2 \rightarrow C_6H_{12}O_6 + 6O_2 \quad (4)$$

1.2 From photosynthetic bacteria to stromatolites

Microbial communities form complex assemblages that are often found bound together by biologically produced extracellular polymeric substances (EPS) to form a biofilm, and in more favourable conditions, they may form a microbial mat visible to the naked eye. Under such conditions, bacteria exert significant chemical control over their local environment, and can drive the precipitation of different kinds of minerals, primarily carbonates, phosphates, sulfates, sulfides, and metal oxides, in a process called biomineralisation (see Konhauser, 2007). As stromatolites are formed almost exclusively by carbonate biomineralisation (combined with grain trapping), only this biomineralisation mechanism is explained here.

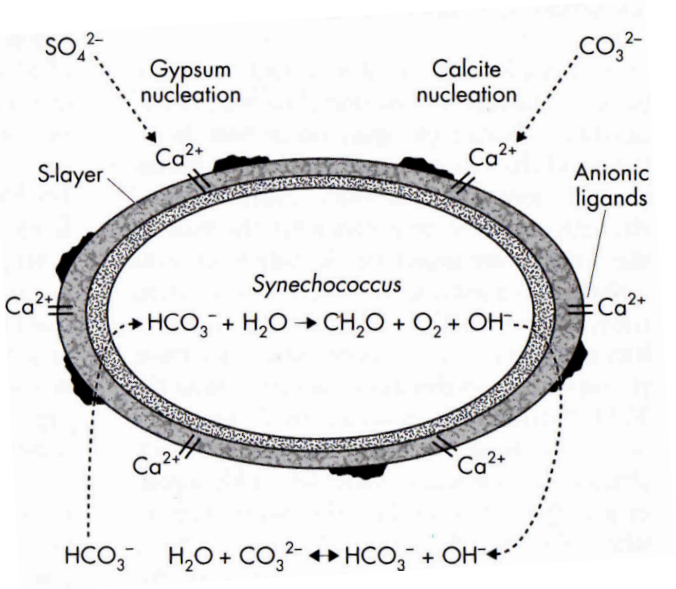

Figure 2.4: Schematic of carbonate biomineralization by cyanobacteria. From Konhauser (2007), adapted from Thompson and Ferris (1990).

The net result of cyanobacterial calcification is the uptake of HCO_3^- from water and export of base (OH^-), resulting in a net increase in proximal pH that ultimately favours carbonate precipitation (see Figure 2.4; Thompson and Ferris, 1990). Bacteria further promote carbonate precipitation by binding metallic cations (e.g., Ca^{2+}) on their external wall and locally increasing the carbonate saturation state. It was shown that the cyanobacteria generator of ESP precipitate more $CaCO_3$ than other organisms (Pentecost, 1978).

At marine pH, the net calcium carbonate precipitation reaction simplifies to:

$$2HCO_3^- + Ca^{2+} \rightarrow CaCO_3 + CO_2 + H_2O \qquad (5)$$

Photoferrotrophic and phototrophic sulphur bacteria similarly favour the precipitation of

carbonate minerals by Ca^{2+} adsorption and uptake of CO_2 (c.f. reactions 1–3; e.g. Hegler et al. 2008). The carbonate produced accumulates as an encrustation on the cell and can lead to a visible build–up of calcite carbonate, and ultimately, to the formation of microbial carbonate structures such as stromatolites. Photosynthetic activity is often associated with daily or seasonal variations, such that precipitation of $CaCO_3$ may be intense in spring and summer, and may wane during winter, perhaps even leading to periods of dissolution (Thompson and Ferris, 1990). To maintain a favourable environment for growth, phototrophic bacteria will continually migrate up the calcite layer (porous or non-porous) that was most recently precipitated, producing the laminated form characteristic of stromatolites. Such migration and upward growth may be modulated by different parameters, including irradiance, tides, changes in salinity, and sedimentation rates (e.g. Chaftez et al., 1991, Konhauser et al. 2001). Heterotrophic organisms are ubiquitous throughout and metabolize the available organic matter, such as dead cells and abandoned EPS. Stromatolites exist in various forms (e.g., millimetre to metre scale, domal, flat, etc), and are the most common type of microbialite. Others include travertine, thrombolites, speleothems, and yet other morphologies that remain poorly classified. In short, stromatolites are directly linked to photosynthetic bacterial activity; this makes them ideally suited for capturing environmental signatures of oxygenic or anoxygenic photosynthesis.

1.3 Molybdenum as a redox proxy

1.3.1 Molybdenum geochemistry

Molybdenum (Mo), transition metal number 42, has seven stable isotopes from mass 92 to 100, namely ^{92}Mo, ^{94}Mo, ^{95}Mo, ^{96}Mo, ^{97}Mo, ^{98}Mo, and ^{100}Mo. Depending on environmental redox conditions, Mo is present in different oxidation states. In oxic conditions (such as in modern seawater), Mo is present in the highly stable molybdate oxyanion form, MoO_4^{2-}. In water with free HS^- (euxinic conditions), sulfidation of MoO_4^{2-} replaces O with S and forms a variety of thiomolybdate ions with the general formula $MoO_{4-x}S_x^{2-}$ (Helz et al., 1996). These properties render Mo highly sensitive to varying redox conditions. Helz et al. (1996) demonstrated total fixation of Mo in marine sediments above a critical H_2S_{aq} concentration of 11 μM, a so-called "geochemical switch". Mo is also an essential micronutrient and is required for many biological activities and metabolic processes (Mendel, 2005). It is one of most abundant transition metals in modern oceans (~100 nM; Collier, 1985), and is well-mixed with a residence time of ~800ky (Emerson and Huested, 1991). Seawater is thus a significant Mo reservoir on the modern Earth. The oxidative weathering of sulfur minerals in the continental crust is an important source of Mo, which is carried

to the ocean by riverine transport with typical dissolved concentrations around 5 nM (Figure 2.5; Morford and Emerson, 1999). Mo displays highly mobile behaviour during weathering, erosion, and transport under oxidizing surface conditions (Siebert et al., 2003). Moreover, low-temperature hydrothermal input is around only 10% of the riverine concentration (McManus et al., 2002). There are two major sinks for Mo in the oceans. The largest sink in the modern oceans are manganese (Mn) oxide minerals (and to a lesser extent, Fe oxide minerals), which bind and highly concentrate Mo by adsorption (Barling et al., 2001; Goldberg, 1954). The second major sink is anoxic sediments, which trap the Mo released by after Fe-Mn oxide reduction by the precipitation of MoS_2. Its concentration in anoxic sediments is typically around 100 ppm (Scott et al., 2008), whereas it averages around 1.1 ppm in the continental crust (Rudnick and Gao, 2003). Anoxic sediments precipitate more rapidly than Fe-Mn-oxide crusts, such that their expansion can easily perturb the balance of Mo sinks. Finally, while molybdenum may be found in carbonates as a trace constituent, carbonates represent only ≤1% of the total marine Mo sink (Morford and Emerson, 1999; Voegelin et al., 2009).

1.3.2 Molybdenum isotopes

Over the past 50 years, the stable isotope compositions of light elements such as carbon and oxygen have proven to be rich paleo-tracers. With the development of multiple collector plasma source mass spectrometry (MC-ICP-MS), isotope geochemists were able to shift focus to transition metals (McManus et al., 2002). Molybdenum isotopic compositions of modern and ancient samples have received significant attention due to their strong potential for paleo-redox reconstruction (Archer and Vance, 2008; Arnold et al., 2004; Barling et al., 2001; Barling and Anbar, 2004; McManus et al., 2002; Planavsky et al., 2014b; Siebert et al., 2003; Voegelin et al., 2009; 2010).

Mo isotopic compositions are represented in the conventional δ notation:

$$\delta^{x/95}\mathrm{Mo} = \left[\frac{\left(\frac{^{x}Mo}{^{95}Mo}sample\right)}{\left(\frac{^{x}Mo}{^{95}Mo}standard\right)} - 1\right] \times 1000 \text{ ‰}$$

Mo isotopic compositions have been primarily reported in two different ways in literature. The most common reporting is $\delta^{98/95}$Mo with respect to the isotope standard "Bern-Mo" (Johnson Matthey ICP standard, lot 602332B; McManus et al., 2002; Siebert et al., 2003; Voegelin et al., 2009; 2010). The second one most common reporting is $\delta^{97/95}$Mo with respect to Roch-Mo2 (Johnson Matthey Specpure Molybdenum Plasma Standard, lot 7024991; Barling et al., 2001; Barling and

Anbar, 2004). Despite this apparent complexity, it is relatively easy to convert from $\delta^{98/95}Mo$ to $\delta^{97/95}Mo$ with a simple multiplication factor of 2/3 (Archer and Vance, 2008), corresponding to the relative mass difference between these notations. The NIST SRM 3134 Mo standard was proposed by Greber et al. (2012) in order to enable easier data comparisons between studies. Goldberg et al. (2013) calibrated the NIST SRM 3134 standard relative to Roch-Mo2 and Bern-Mo:

$$\delta^{98/95}Mo_{SRM\ 3134} = \delta^{98/95}Mo_{Roch\text{-}Mo2} + 0.34 \pm 0.05\ ‰$$
$$\delta^{98/95}Mo_{SRM\ 3134} = \delta^{98/95}Mo_{Bern\text{-}Mo} + 0.27 \pm 0.06\ ‰$$

^{98}Mo or ^{97}Mo are heavier than ^{95}Mo (97.9 u and 96.9 u vs. 94.9 u). In delta notation, if $\delta > 0$, the sample is enriched in heavy isotopes relative to the standard (is isotopically heavier). On the other hand, if $\delta < 0$, the is enriched in light isotopes relative to the standard (is isotopically lighter). At $\delta=0$, the sample has the same isotopic composition as the standard.

Siebert et al. (2003) was first to constrain mean ocean $\delta^{98/95}Mo$, reporting an isotopically heavy value of 2.63‰ ± 0.1(2σ). This value now serves as the reference for dissolved Mo in mean ocean water (MOMo; Figure 2.2). An even heavier isotopic composition was measured by McManus et al. (2002) for deep marine sediment pore waters, where isotopically light Mo (relative to seawater) accumulates in reducing sediments (the most important marine sink), leaving a low concentration of heavy residual Mo in associated pore waters.

All Mo sources and sinks have a lighter isotopic composition than seawater (Figures 2.5 and 2.6). The isotopic offset between oxic and anoxic sediments is fixed by the isotopic composition of the most important Mo source, that being river water (Figures 2.5 and 2.6; see also Arnold et al. (2004) for a Mo isotope mass balance model).

The heavy Mo isotopic composition of seawater is thus entirely explained by reduced sediments, which have a light isotopic composition and are the most important marine sink of Mo (McManus et al., 2002; Siebert et al., 2003). The second most important sink, Fe-and Mn-oxide-rich sediments, represents an even lighter Mo isotope exit channel, but is less important today than the reduced sedimentary sink (Arnold et al., 2004). The Mo isotopic composition of carbonates is assumed to have an insignificant affect on the Mo isotopic composition of seawater because they contain very little Mo and are thus relatively unimportant from a mass-balance compared to the major sources and sinks identified. Furthermore, it appears that Mo is unfractionated from seawater during incorporation into carbonates (see below).

When Mo removal from seawater is quantitative, the Mo isotope composition of reducing sediments may be directly linked to the isotopic composition of contemporaneous seawater, and in turn, to the relative importance of reducing and oxic areas of the seafloor. Using a conservative

assumption of 70% Mo removal by euxinic sediments in the mid-Proterozoic, Arnold et al. (2004) used simple isotope mass balance to calculate the isotopic composition of mid-Proterozoic seawater to be around 1.5‰. In the same manner, mid-Proterozoic riverine inputs have been estimated to be around around 1‰ (Archer and Vance, 2008).

The above calculations require near quantitative Mo removal into the ancient sediments upon which these estimates are based. Carbonate sediments appear to hold significant promise in this regard. A recent study examining modern carbonate samples has shown that non-skeletal carbonates present a $\delta^{98/95}$Mo close to seawater, whereas skeletal carbonates show a Mo isotopic composition that is only slightly lighter (between 1.96 and 2.59‰; Voegelin et al., 2009). Contrary to modern euxinic sediments, highly localized in basins, carbonate sediments appear better to record global seawater Mo isotope compositions. Voegelin et al., (2010) demonstrated this assumption by the examination of Archean shale and carbonate records. The maximal $\delta^{98/95}$Mo value measured on Archean carbonates seems to be a reliable and direct reflection of the $\delta^{98/95}$Mo value of contemporaneous seawater (determined by Voegelin et al. (2010) to be upwards of 1.3‰ ca. 2.52 Ga).

As all major isotope exchange reactions of Mo depend directly of the MoO_4^{2-} molecule, any isotope fractionation of Mo from crustal values requires the presence of oxygen.

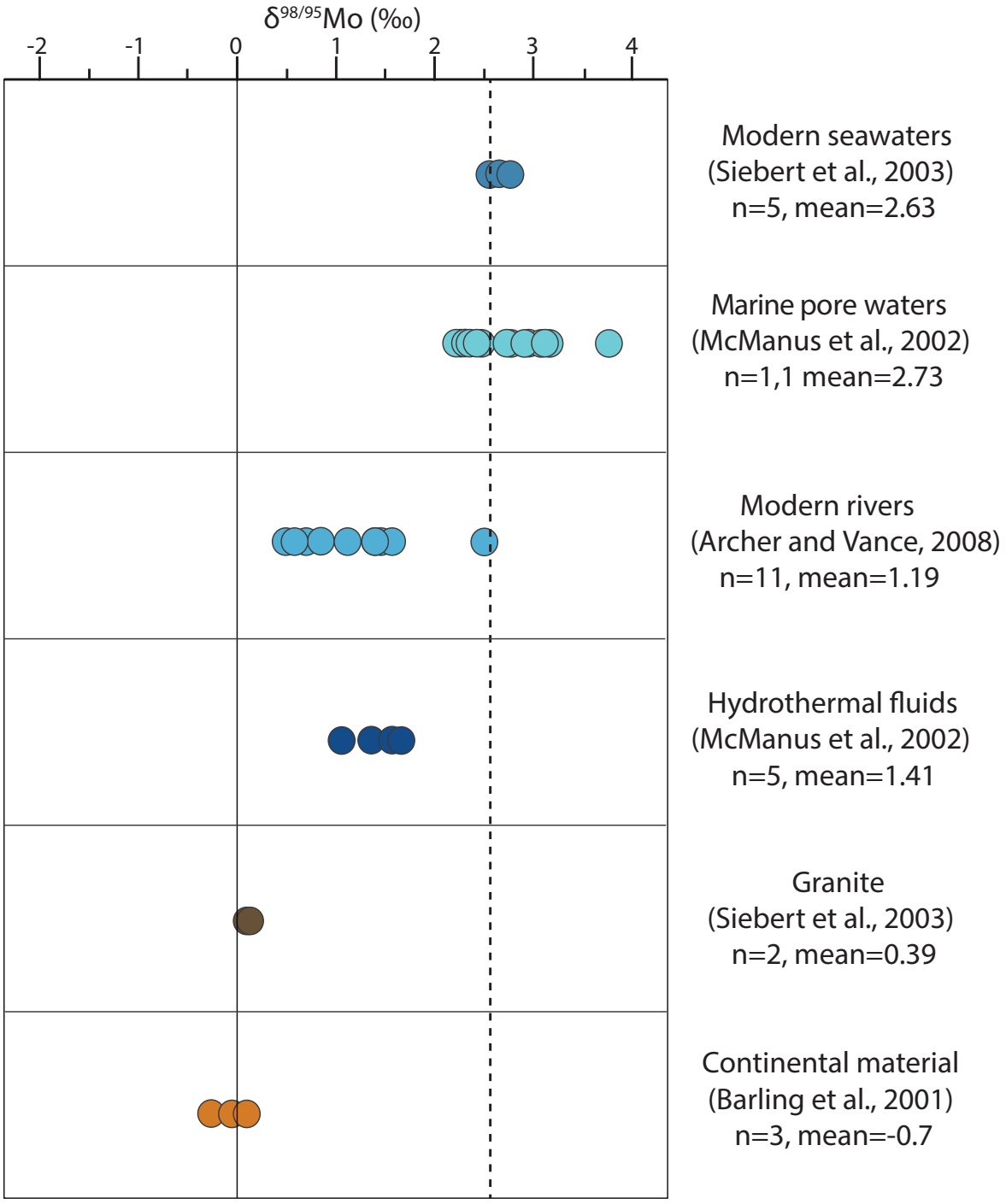

Figure 2.5: Compilation of Mo isotopic signature of Mo sources of seawater. The mean of modern seawater and crust Mo isotopic signature are represented by respectively a dash line and a full line.

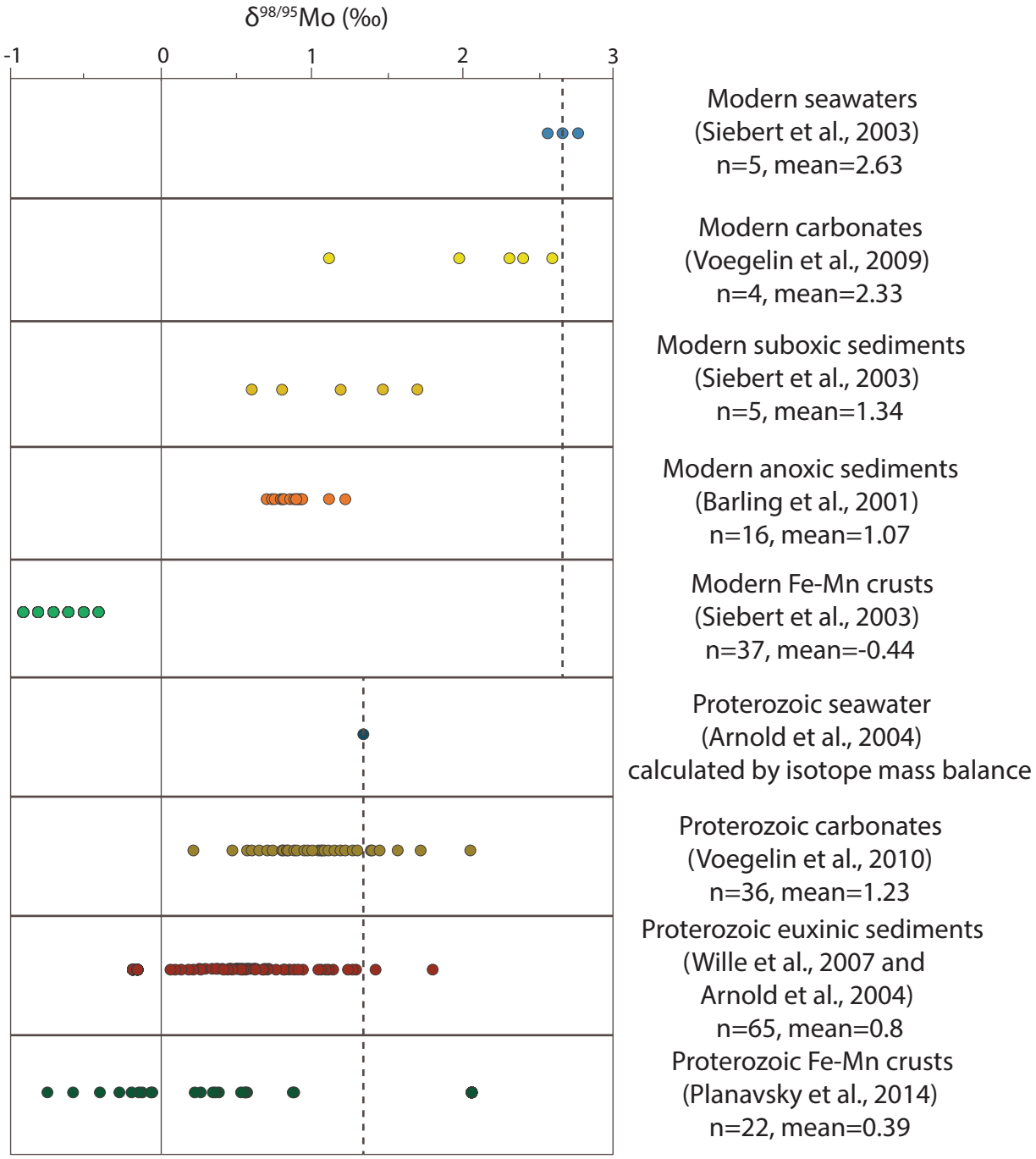

Figure 2.6: Compilation of Mo isotopic signature of Mo sinks of seawater. The mean of modern and Proterozoic seawater and crust Mo isotopic signature are represented by respectively two dash lines and a full line.

2. Materials and Methods

2.1. Materials

In order to compare the Mo isotopic signature of modern and ancient stromatolites and microbialites, measurements of the Mo isotopic composition of 18 samples were realised: 5 modern stromatolites, 11 ancient stromatolites, and 2 ancient microbialites.

Modern stromatolites (n=5) from the Bacalar Lagoon, Mexico, were provided by Dr. Kurt Konhauser (University of Alberta). Bacalar is a marl lagoon, with sediment composed of >35% carbonate, aragonite, and clay (LaBuhn et al., 2012). It's clear freshwater is compositionally homogenous except in the cenote, which is poor in dissolved oxygen. The majority of the stromatolites growing there were built by cyanobacteria in the late Holocene following a rise in carbonate concentration in the lagoon. This carbonate came from dissolution of the underlying Cenozoic limestone karst system (Gischler et al., 2008). The stromatolites are growing even today despite an invasion of mussels.

The ancient stromatolites come from two different Archean cratons. The oldest ones (n=3) are from the Red Lake carbonate platform, Canada, and are 2.96 Ga years old. They were kindly provided by Dr. Philip Fralick (Lakehead University). They grew in shallow carbonated water on a felsic volcanic section (Thurston and Chivers, 1990). Two other stromatolites (one digitate and one flat, also from Philip Fralick's collection) and two microbialites were also analyzed from the 2.8 Ga years old Steep Rock locality. They belong to the Mosher Carbonate unit, which is composed of calcite, ankerite, and dolomite, with minor quartz, pyrite, and kerogen. The Steep Rock stromatolites were discovered in 1913 by Lawson and can be up to 16.5 meters tall (Wilks and Nisbet, 1985). Multiple forms of stromatolites grew here in shallow tidal water environments, perhaps lagoonal and/or shelf settings close to a shallow sea. A stratigraphic analysis of the Steep Rock stromatolites and of their different forms suggests an environment with a subsiding basement, or possibly a eustatically transgressed basement (Wilks and Nisbet, 1985). The other five ancient stromatolite samples are from a second craton, specifically from the Gamohaan formation, South Africa. Dated at 2.52 Ga by Sumner & Bowring (1997), this formation is in the Ghaap group, Griqualand West Basin. They were kindly provided by Dawn Summer (UC Davis). These stromatolites were built in deep subtidal water, in a sub-wave-base environment (Sumner, 1997).

2.2. Principles of Mo isotope measurement

2.2.1. MC-ICP-MS

Isotopic measurement of transition metals by multiple collector plasma source mass spectrometry (MC-ICP-MS) has only been possible late in the last century (Halliday et al., 1995). Its principle is straightforward (Annex 1): ions of the isotopes of interest are formed when the sample is nebulised and carried in the form of a mist into a high-temperature plasma, usually argon gas-based. They are separated from each other as a function of mass in two steps: a) an electric sector that filters based on kinetic energy, and b) a magnetic sector that deflects isotopes based on their mass, where the lighter isotopes are deflected more than the heavy ones. Once the isotopes are separated, an array of multiple collectors captures all of the isotopes simultaneously and the signal is measured.

2.2.2. Sample preparation

Mo, a transition metal, is everywhere around us (especially as a dopant in steel). That is why all of the sample preparation for molybdenum isotope measurements should be performed in a clean room with a particulate attention of metal contamination. The sample needs to be in solution to be analysed. Rock samples are first powdered and then the powder is digested to extract the element under investigation. The goal of this research was to study authigenic molybdenum in carbonates and examine its isotopic signature. Accordingly, the digestion would ideally be delicate, e.g. as part of a leaching procedure (e.g., in 5% acetic acid). However, Voegelin et al. (2009) showed that seawater Mo isotope signatures are retrieved from carbonate even with a "pseudo-total" 6N HCl attack.

The final solution to be passed through the spectrometer should be concentrated and purified to eliminate potential interferences and remove potential matrix effects. Column chromatography is a robust way to achieve this goal. Its principle is based on the solubilisation of mobile phases and the retention of stationary phases as a function of their affinity to an exchange resin. Such resins are generally composed of polymer beads with functional groups grafted to them. These groups should retain or release ions as a function of solution chemistry. If the mobile ion is positive, the resin undergoes a "cation exchange", and if the mobile ion is negative, the resin undergoes an "anion exchange", which has a positive functional groups positive to attract negative mobile ions. With elution, charged elements in the resin are separated due to different migration speeds.

2.2.3. The isotope double spike method

An isotope double spike method was used to correct for isotopic fractionation induced during the sample preparation and MC-ICP-MS analysis (Rudge et al., 2009; Siebert et al., 2001). It consists of an addition to the sample of two purified isotopes of the element interest at roughly the same concentration as the natural isotopes in the sample. Both spiked isotopes should have relatively little natural abundance and be free of isobaric interference (other potential signals of the same mass). In the case of Mo, ^{97}Mo and ^{100}Mo have been used, which have relative natural abundances of 9.55% and 9.63%, respectively. ^{97}Mo has no major isobaric interferences, while ^{100}Mo may be interfered by ^{100}Ru. This interference can easily be accounted for through correction using measurement of ^{99}Ru measurement. Contrary to unspiked methods, the double spike method can offer superior precision and controls for any potential fractionation that might occur during sample preparation.

Using the double spike method, $\delta^{98/95}$Mo values must be iteratively calculated from measurements of the mixture (Siebert et al., 2001, Rudge 2009). Two different methods have been suggested in the literature: a matrix solution as detailed by Rudge et al. (2009) and a geometrical calculation as detailed by Siebert et al. (2001). These calculations yield multiple isotope ratios (in this case, ^{100}Mo/^{98}Mo, ^{97}Mo/^{98}Mo, and ^{95}Mo/^{98}Mo) of the samples and standards, and permit the determination, to a high precision, of instrumental and natural sample fractionation. Finally, $\delta^{98/95}$Mo is expressed according to the following equation:

$$\delta\,^{98/95}\mathrm{Mo} = \left[\frac{\left(\frac{^{98}\mathrm{Mo}}{^{95}\mathrm{Mo}_{\mathrm{sample}}}\right)}{\left(\frac{^{98}\mathrm{Mo}}{^{95}\mathrm{Mo}_{\mathrm{standard}}}\right)} - 1\right] \times 1000 \text{ ‰}$$

For international comparability, the standard used should be accepted by the wider research community, for a $\delta^{98/95}$Mo standard value of 0 across all studies. In the case of $\delta^{98/95}$Mo, the standard usually used is NIST SRM 3134 (Goldberg et al., 2013; Greber et al., 2012). Nevertheless, a homemade (internal) standard may be used for measurements, as long as calculations to correct for deviations from the international standard are also made.

2.3. Methods of this study

All experiments were conducted in the PSO class 1000 clean labs at IFREMER, Brest, France. To determined the most effective method for sample dissolution, preliminary tests were

made on large quantities of 0.64 Ga carbonates from Brazil (courtesy of Pierre Sans Jofre): 1) a weak leach attack and 2) a ("pseudo-") total attack. The weak leach was completed using 5% acetic acid, similar to the protocol used by Rongemaille et al. (2011). The abundance of Mo extracted from the carbonates using this simple leaching technique was found to be too low for Mo isotope analyses (Figure 3.1). Therefore, the total attack method was deemed more appropriated (Voegelin et al., 2009). This method uses 6N HCl and a few drops of H_2O_2 to dissolve the carbonate and keep Mo in its highly soluble Mo^{6+} oxidation state. The samples were then placed on a hot plate at 80°C for 24 h in order to aid dissolution (Voegelin et al., 2009).

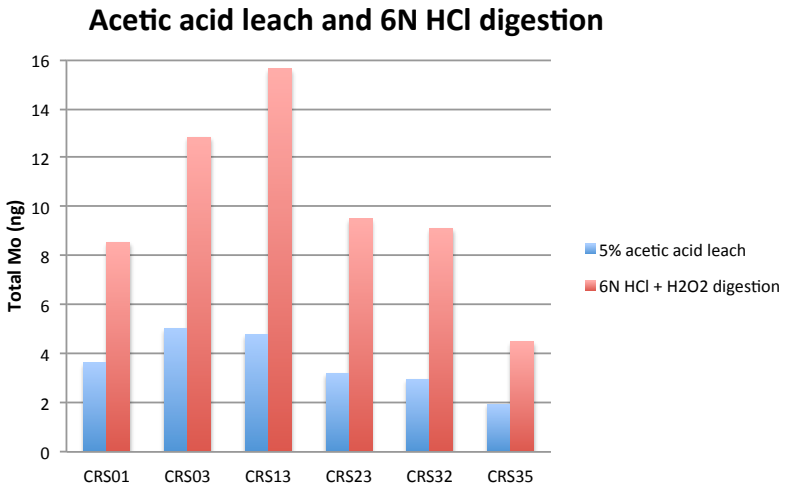

Figure 3.1: Measurement of Mo concentration by double spike isotope dilution using the MC-ICP-MS Neptune on different carbonate samples (CRS). Red columns: measurement after a total attack with 6N HCl according to the protocol of Voegelin et al. (2009). Blue columns: measurement after a weak leach by 5% acetic acid according Rongemaille et al. (2011).

Once the total attack was completed, samples were centrifuged (4000 rpm, 6 min) in order to isolate the liquid phase (residues were stored for future analyses). 200 µL of the total volume was diluted in 8mL of 2% HNO_3 doped with 2 ppb Indium for preliminary analysis of Mo concentrations by the HR-ICP-MS Element 2 (PSO-Brest). Natural ^{97}Mo concentrations (with no isobaric interferences) were measured at high and medium resolution. These measurements were drift-corrected using the 2 ppb Indium present in all solutions (samples standards, and rinses), and concentrations were defined by the relation between detector counts and known concentrations of in-house certified solutions prepared at different concentrations.

Once preliminary analyses determined approximate Mo concentrations, samples were double spiked at the same concentration using a ^{97}Mo+^{100}Mo double spike (DS) in order to achieve a DS/natural Mo concentration ratio of 1. Spiked samples were then passed through two chromatographic columns. The first contained 1 ml of anion exchange resin (AG1-X8) and the second contained 1 ml of cation

exchange resin (AG50W-X8). Samples were purified according to the protocol of Asael et al. (2013) as detailed in Annex 2. To validate the Mo elution procedure, Mo from different certified standards were isolated by column chromatography and concentrations at each column step were evaluated using HR-ICP-MS Element 2 for Mo and using ICP-AES for major elements. Three different samples were used for column calibration: SDO-1 (a Devonian shale from Ohio), Mo SPEX at 1 ppm (in-house standard), and a mixture of SPEX+CAMIL32, a Neoproterozoïc carbonate from Brazil doped with Mo to investigate the influence of the carbonate matrix on the chromatographic procedures. Mo elution profiles for each standard are shown in Figure 3.3, and confirm good recovery of Mo from both columns.

sample		1ml HCl 6N
matrix	1 2	HCl 6N (2X3ml)
Mo	1 2 3	HNO_3 2N (3X3ml)

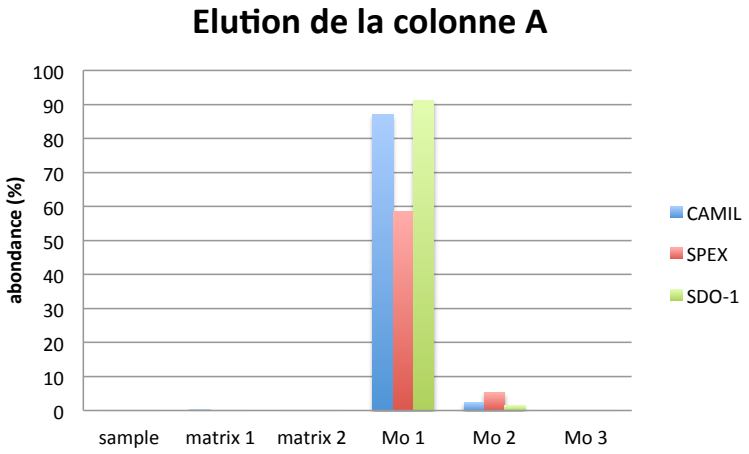

sample		1ml HCl 0.24N
Mo	1 2 3	HCl 0.24N (3X3ml)
Fe	1 2	HCl 6N (2X3ml)

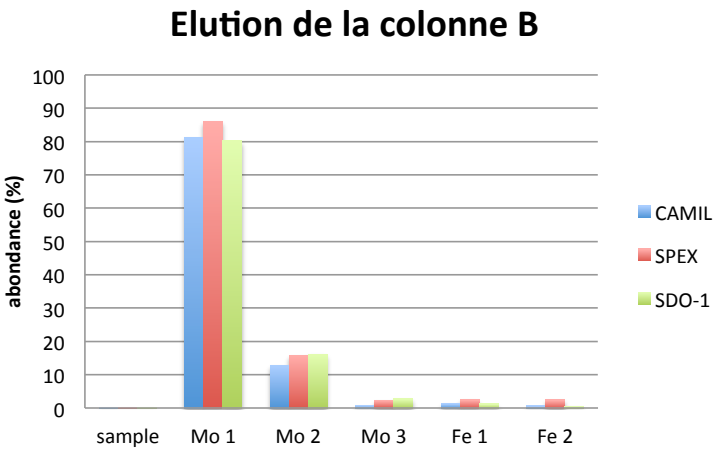

Figure 3.2: Elution of molybdenum from SDO-1, SPEX, and SPEX-CAMIL32 column tests. Measurements were performed by HR-ICP-MS (see Annex 2).

The first column (anion exchange) was relatively effective with Mo yields between 64% and 93%, and the second one was better with yields between 97% and 107% (Figure 3.4). Instrumental errors were estimated at 3.43% (2 RSD). Note that the poor yield in both cases was from the SPEX standard, a solution without rock matrix.

Abondance	Colonne A	Colonne B	2σ
CAMIL	90 %	97 %	3.43
SPEX	64 %	107 %	3.43
SDO-1	93 %	107 %	3.43

Figure 3.3: Mo yields through both chromatographic columns used to concentrate and purify molybdenum.

Regarding major element elution profiles analyzed by ICP-AES, only the iron comes out in the same fraction as the Mo in the first column, and is effectively separated during the second column step (Figure 3.5). Thus the double column procedure effectively separates molybdenum from carbonate matrices. Mo yields are not perfect, but the double-spike method inherently corrects for any potential isotope fractionation that may occur on the columns.

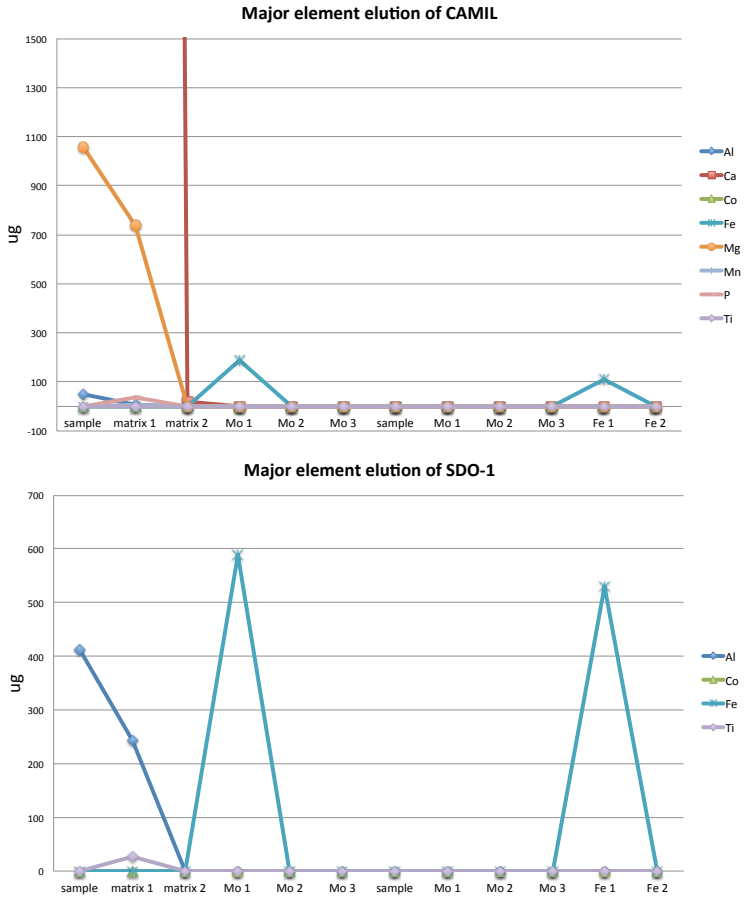

Figure 3.4: Elution of major elements in the SDO-1 and Camil elution tests. Measurements were performed by ICP-AES.

2.4. Mo isotopic measurements

After samples were passed through both columns, they were diluted with 2% HNO3 for

analysis on the MC-ICP-MS Neptune (IFREMER; Annex 1). A desolvating nebuliser with temperature-controlled spray chamber (APEX–Q) was used for all measurements. Instrument tuning was performed with 100 ppb SPEX-DS solutions. First, samples were analyzed to determine their Mo concentrations after column separation. Samples were then diluted to a final Mo concentration of 100 ppb, consistent with the concentration of the standard (100 ppb SPEX-DS). Finally, every sample was analysed with 30–50 acquisitions on Mo masses 92, 94, 95, 96, 97, 98, and 100.

The data points were subsequently broken into blocks of five, and the mean of all blocks was determined. Blocks were considered as outliers if they differed by two standard deviations or more from the mean. All signals were blank-subtracted. The final DS/Nat ratio was determined by double spike calculation and only samples with DS/Nat ratios under 15 were considered further, although isotope ratios appeared unaffected at high DS/Nat ratios (Annex3). Iterative double spike calculations were performed according to the geometric system of Seibert (2001) using the isotope ratios 95/98Mo, 97/98Mo and 100/98Mo (Siebert et al., 2001). $\delta^{98/95}$Mo is the determined in delta notation by the equation:

Repeated SPEX measurements should be stable (Figure 3.4) and their daily averages were used to in the final calculation of δ^{98}Mo values. Repeated method blanks had Mo concentrations between 0.5ng and 2.58 ng of Mo. To be universally comparable, results were transformed from SPEX to SRM standardizations. According to Asael et al., (2013), the in-house SPEX standard is indistinguishable within error from the Roch-Mo2 standard:

$$\delta^{98/95}Mo_{SPEX} = \delta^{98/95}Mo_{Roch\text{-}Mo2} - 0.05 \pm 0.06\ ‰$$

No correction was made in this first step, but all results were then reported relative to SRM3134 as per (Goldberg et al., 2013):

$$\delta^{98/95}Mo_{SRM\ 3134} = \delta^{98/95}Mo_{Roch\text{-}Mo2} + 0.34 \pm 0.05\ ‰$$

3. Results

Considering the potential for isobaric interference (e.g.,^{98}Mo by ^{98}Ru), a plot $\delta^{95/98}$Mo vs $\delta^{97/98}$Mo (after double spike calculation) had to be checked in order to verify interference-free measurements of all isotopes (e.g., as per Rouxel et al. (2006)). All data yield a straight line, indicating strictly mass-dependant fractionation and interference-free measurement of molybdenum isotopes (Figure 4.1).

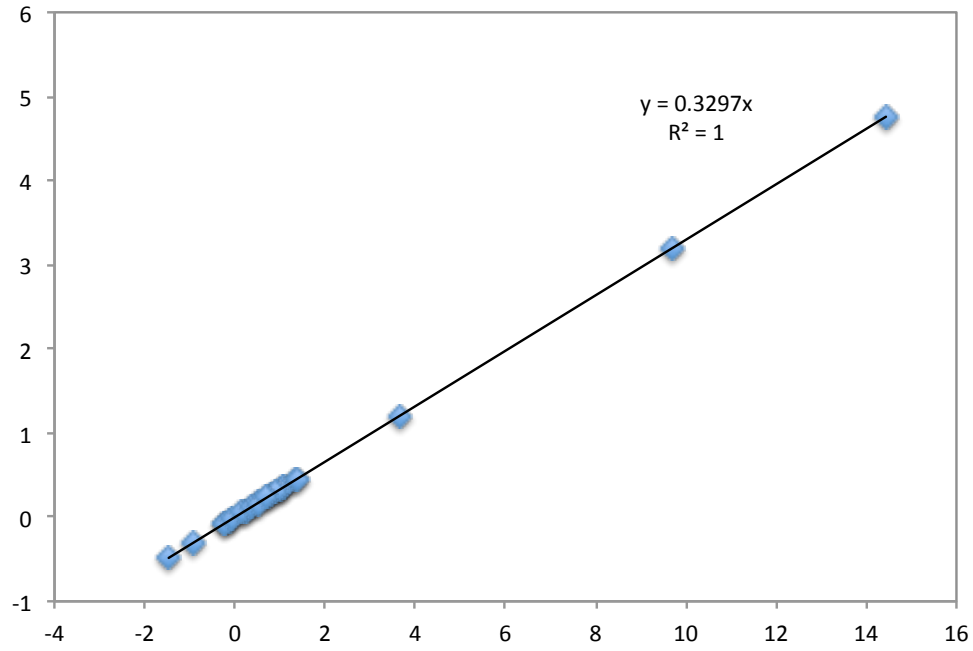

Figure 4.1: Correlation between δ95/98Mo and δ97/ 98Mo with a slope equal to the relative mass differences of 97Mo/98Mo (1) and 95Mo/98Mo (3) support an isobaric interference-free measurement of all these isotopes.

No correlation was observed between δ^{98}Mo and the DS/Nat ratio, suggesting reliable δ^{98}Mo measurement at DS/Nat<15 (Annex 3a). Moreover, no correlation exists for most samples between δ^{98}Mo and the Mo concentration (Annex 3b), implying a lack of detrital contamination. If detrital contamination were prevalent, higher Mo concentrations would be accompanied increased detrital Mo that would push δ^{98}Mo towards the crustal isotope composition of 0.

Mo concentration and isotopic composition data for modern and ancient stromatolites are listed in Table 1.

Description	Age (Ga)	Name	Nature	Concentration (ppb)	DS/Nat	$\delta^{98/95}Mo_{SPEX}$	2σ	$\delta^{98/95}Mo_{SRM\ 3134}$	2σ
Bacalar, Mexico	0	Sed Bacalar 2011	Stromatolite	6.15	6.29	1.21	± 0.15	**1.55**	**± 0.15**
		110326/2 Top	Stromatolite	7.73	11.75	0.80	± 0.15	**1.14**	**± 0.15**
		core1-21	Stromatolite	13.88	11.88	0.46	± 0.08	**0.80**	**± 0.08**
		110326/2 Middle A	Stromatolite	12.31	11.90	0.26	± 0.11	**0.60**	**± 0.11**
		core1-27	Stromatolite	8.55	12.71	0.45	± 0.07	**0.79**	**± 0.07**
		core1-29	Stromatolite	12.09	12.99	0.46	± 0.11	**0.80**	**± 0.11**
		mean		**10.12**		**0.61**	**± 0.11**	**0.95**	**± 0.11**
Gamohaan, South Africa	2.52	KU9DS01Abis	Stromatolite	35.50	2.31	-0.25	± 0.14	**0.09**	**± 0.14**
		KU100DS01A	Stromatolite	51.30	2.64	-0.24	± 0.12	**0.10**	**± 0.12**
		KU100DS01B	Stromatolite	50.92	3.10	-0.10	± 0.07	**0.24**	**± 0.07**
		ALI-DS-82D	Stromatolite	45.42	3.75	0.24	± 0.07	**0.58**	**± 0.07**
		KU9DS01A	Stromatolite	40.18	3.88	-0.09	± 0.10	**0.25**	**± 0.10**
		KU9DS01B	Stromatolite	25.08	6.98	0.52	± 0.14	**0.86**	**± 0.14**
		mean		**41.40**		**0.01**	**± 0.11**	**0.35**	**± 0.11**
Steep Rock, Canada	2.8	P-1	Microbialite	54.27	2.21	1.06	± 0.14	**1.40**	**± 0.14**
		P-9	Microbialite	24.62	5.06	1.01	± 0.23	**1.35**	**± 0.23**
		P-10	Stromatolite	32.72	3.78	0.82	± 0.18	**1.16**	**± 0.18**
		P-7	Stromatolite	64.02	3.80	1.06	± 0.11	**1.40**	**± 0.11**
		mean		**40.35**		**0.75**	**± 0.16**	**1.33**	**± 0.16**
Red Lake, Canada	2.96	P-33	Stromatolite	20.45	2.15	-0.91	± 0.08	**-0.57**	**± 0.08**
		P-35	Stromatolite	37.61	3.22	0.71	± 0.16	**1.05**	**± 0.16**
		P-34	Stromatolite	14.06	7.26	0.38	± 0.21	**0.72**	**± 0.21**
		mean		**34.87**		**0.47**	**± 0.15**	**0.40**	**± 0.15**

Table 1: Results of Mo isotopic analyses of modern and ancient stromatolites. δ^{98}MoSRM3134 values were obtained by the addition of 0.34‰ to the RochMo2–normalized values, as per Goldberg et al. (2013).

Mo concentration in the modern stromatolites were generally very low, between 6.5 ppb and 13.88 ppb. Their Mo isotopic compositions ranged from 0.6‰ to 1.55‰, with an average of 0.95‰±0.11‰ (2σ; Figure 4.2).

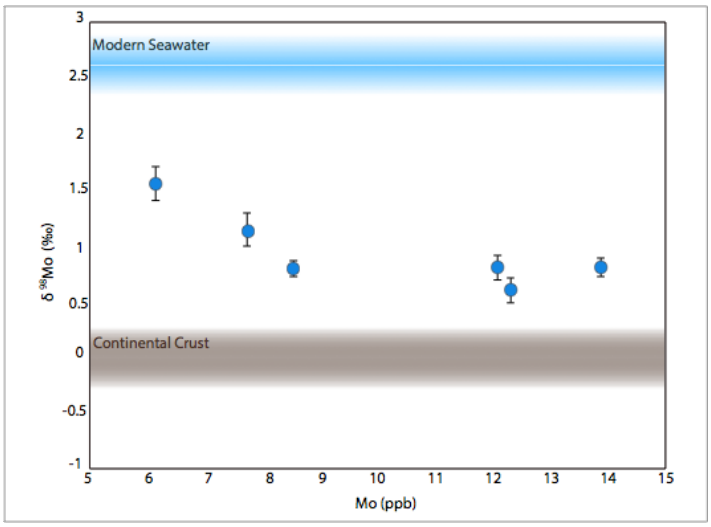

Figure 4.2: δ^{98}Mo and Mo concentrations of modern stromatolites from Bacalar lagoon, Mexico.

Ancient stromatolites from Gamohaan formation, South Africa (2.52 Ga), have higher Mo concentrations with an average value of 41.4 ppb. Their isotopic compositions are among the lowest measured in this study (from ~0‰ to 0.86‰; Figure 4.3).

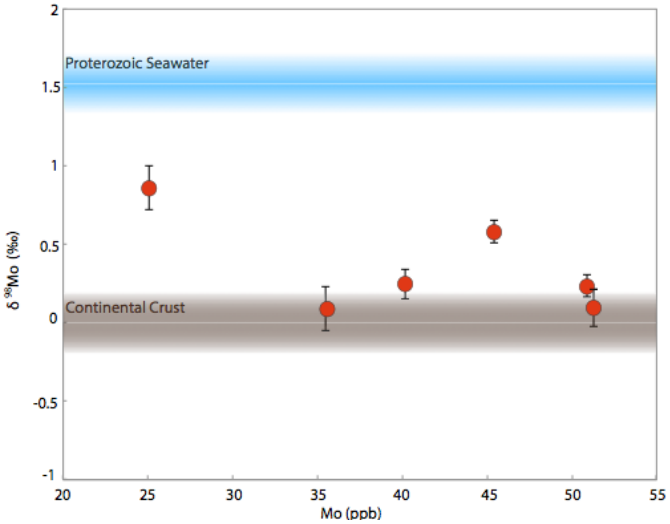

Figure 4.3: δ^{98}Mo and Mo concentrations of ancient stromatolites from the Gamohaan formation, South Africa, 2.52Ga.

The 2.8 Ga stromatolite samples from Steep Rock, Ontario, contained the highest Mo concentrations of the sample set, yielding Mo concentrations between 32.72 ppb and 64.02 ppb (Figure 4.4). Moreover, with isotopic compositions from 1.16‰ to 1.4‰, they are the isotopically heaviest samples of the ancient stromatolites examined in this study. The measured microbialites from Steep Rock show a similar isotopic composition of Mo (1.35‰ and 1.4‰).

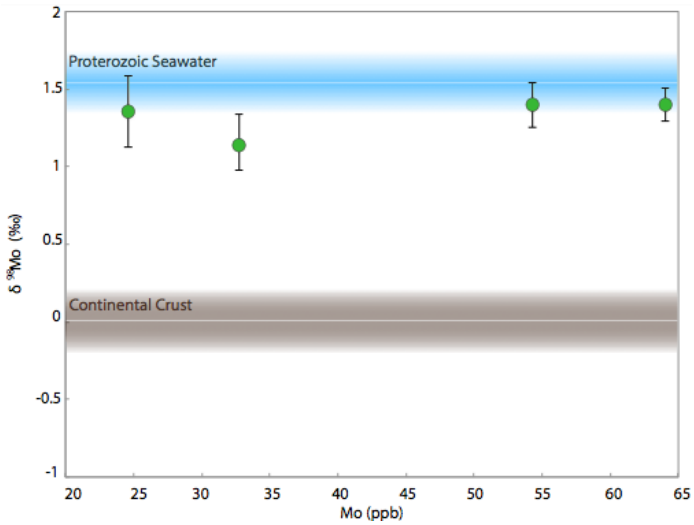

Figure 4.4: δ^{98}Mo and Mo concentrations of ancient stromatolites from Steep Rock, Canada, 2.8Ga.

Finally, the 2.96 Ga stromatolites from Red Lake, Ontario, have the lowest Mo concentrations of ancient stromatolites, with an average of 34.87 ppb (Figure 4.5). Their isotopic compositions show a large variation, from -0.57‰ and 1.05‰. With the exception of sample P-33, (δ^{98}Mo = -0.57 ± 0.08‰, 2σ), the samples have a positive δ^{98}Mo signature (Figure 4.5).

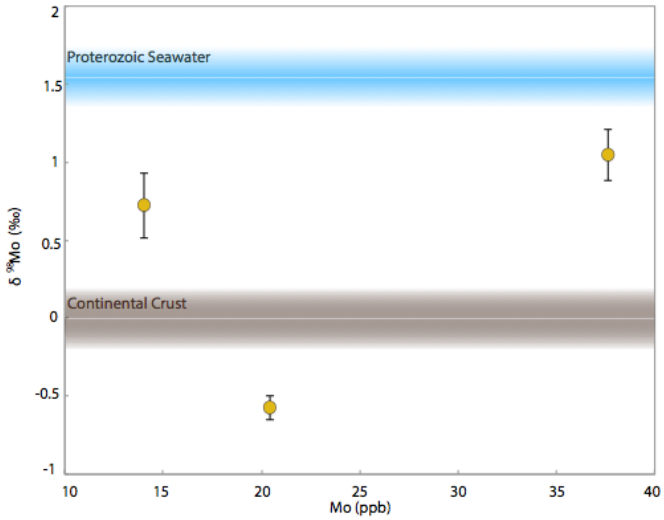

Figure 4.5: δ^{98}Mo and Mo concentrations of ancient stromatolites from Red Lake, Canada, 2.96Ga.

All of modern and ancient stromatolites have δ^{98}Mo values below the contemporary Mo isotopic composition of seawater (Figure 4.2 to 4.5). Except for P-33, with a light δ^{98}Mo composition of -0.57‰ ± 0.08‰ (2σ), all of the sample examined carry a positive δ^{98}Mo signature (Figure 4.6).

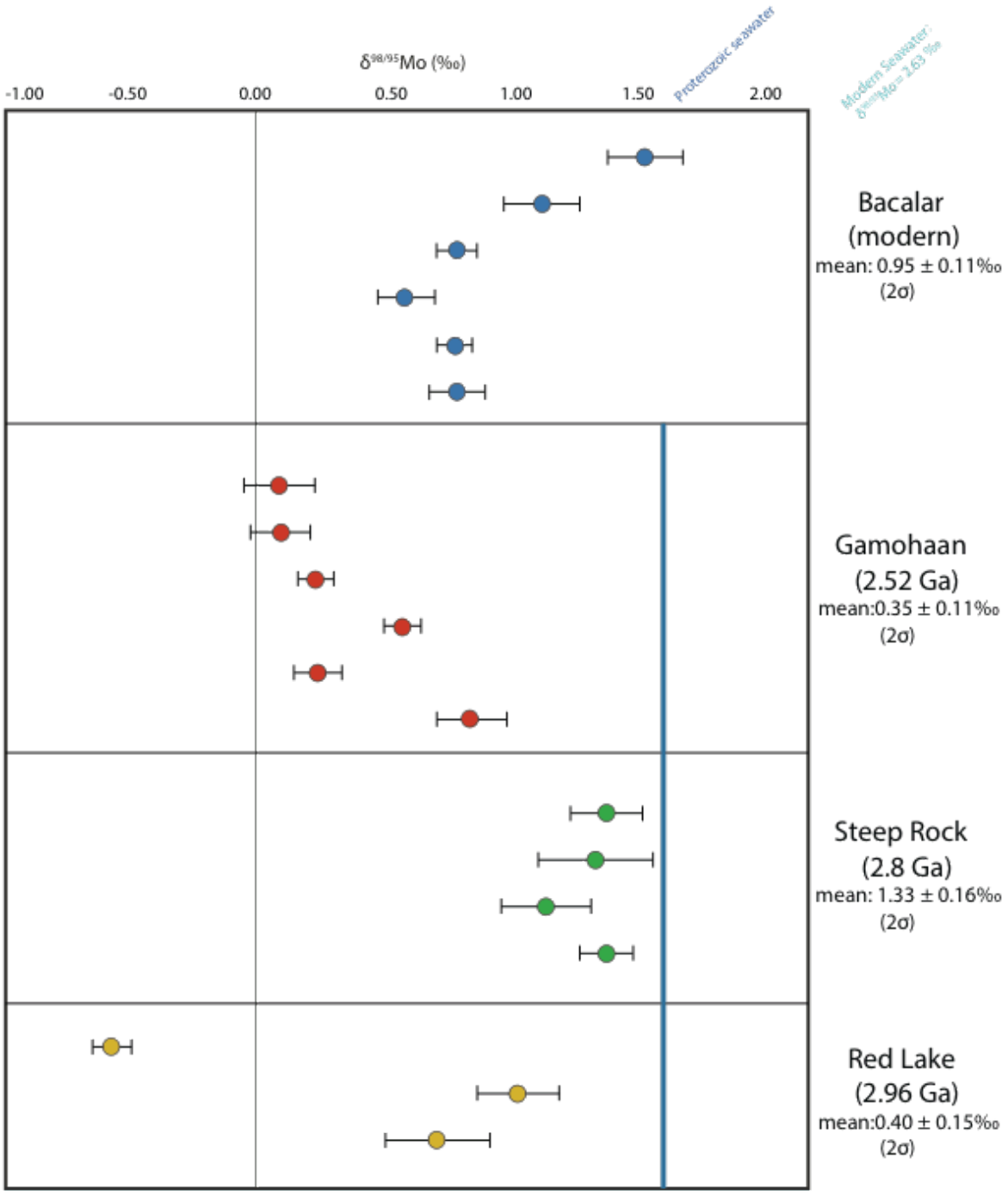

Figure 4.6: $\delta^{98/95}$Mo values of modern and ancient stromatolites examined in this study.

4. Discussion

4.1. Modern stromatolites

Voegelin et al. (2009) reported that the global ocean Mo isotope composition is preserved in non-skeletal carbonates forming from seawater. Bacalar stromatolites, a non-skeletal sample grown in freshwater, present isotopic compositions similar to the modern Mo isotope river array (Figure 5.1; Archer and Vance, 2008). Similar to hydrothermal Mo signature too, they are not springs inside the lagoon; consequently, no relation could be effected between Mo isotopic signature of Bacalar stromatolites and of hydrothermal water. This new example of carbonates from a freshwater lagoon supports the idea that Mo isotope signatures of carbonates, and consequently stromatolites, are unfractionated from their formation waters, and should serve as a good proxy for determining the Mo isotope signature of the water from which they grew, as well as for understanding ancient oxygen production and paleoredox.

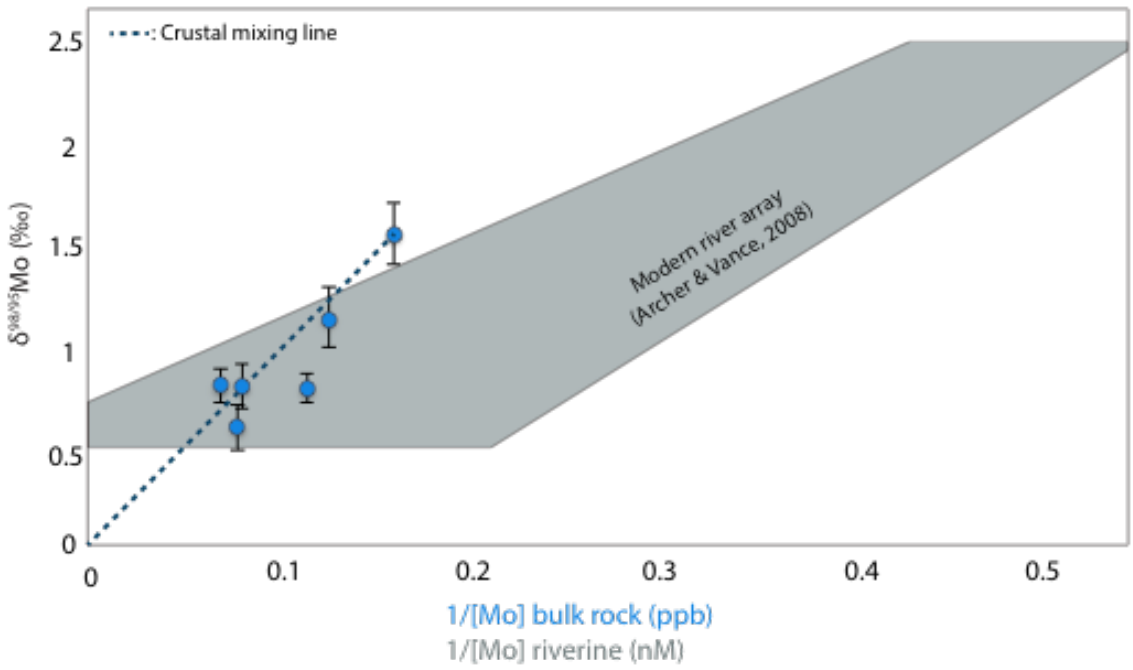

Figure 5.1: Mo isotopic compositions of Bacalar modern stromatolites from this study (blue points) appear to overlap with the modern river array (grey area; Archer and Vance, 2008). However, a mixing model based on the composition of continental crust (δ^{98}Mo=0‰, Siebert et al. (2003) and Mo=1100ppb; Rudnick and Gao (2003)) and the isotopically heaviest stromatolite in this area (δ^{98}Mo =1.55‰ and Mo=6.15ppb) suggests a detrital dependence.

There appears to be a relationship between δ^{98}Mo and 1/[Mo], similar to the "the river water array" (Archer and Vance, 2008), where lower concentrations of molybdenum yield heavier isotopic compositions (Figure 5.1). For the river array, Archer and Vance (2008), proposed two solutions to explain this correlation. The first one considered the role of detrital contributions, whereby the higher concentrations of molybdenum could be induced by increased detrital Mo input and, consequently, result in decreased riverine δ^{98}Mo. The second theory involved the retention of lighter Mo isotopes during transport after sulphide weathering, thereby producing heavy residual waters. To examine for the Bacalar stromatolite data in light of these scenarios, a mixing model was developed between the most Mo-poor Bacalar stromatolite of this study and the continental crust, assuming a crustal Mo concentration of 1100 ppb (Rudnick and Gao, 2003). Even if Bacalar stromatolites fortuitiously plot along modern « the river array », the mixing model reveals a likely dilution of the Mo isotope signal by detrital contamination (Figure 5.1). Moreover, Siebert et al. (2015) shown that the second argument is poorly supported at present and appears dependent of many environmental effects (e.g., climate, organic matter, degree of weathering) that can cause to either light or heavy isotopes of Mo to be retained during weathering. The Bacalar stromatolites nonetheless record fractionated Mo from their environment, and the mixing calculation shows that one can define a "minimum" molybdenum isotopic composition of the formation waters based on the molybdenum isotope composition of the least-contaminated stromatolite grown in this water body.

4.2. 2.52 Ga stromatolites, Gamohaan formation, South Africa

These stromatolites grew in a subtidal environment (Sumner, 1997) and represent the lightest collection of Mo isotopic compositions measured in this study. Their Mo isotopic compositions range from 0.09% to 0.86‰, suggesting a closer association with the continental crust Mo isotopic signature (Figure 5.2). Their relatively unfractionated Mo isotope compositions indicates little free oxygen and thus molybdate (MoO_4^{2-}) production at this time. Bekker et al. (2004) reported an intense sulfur MIF (mass independent fractionation) signal in diagenetic pyrite from the Gamohaan formation, and also reported detrital pyrite and uraninite nearby in the basin. All of these arguments support an anoxic Earth surface environment at this time. Moreover, a negative Ce anomaly in BIF just overlying the Gamohaan formation, and a δ^{34}S value near ≈0‰ for diagenetic pyrite (indicating a small sulfate reservoir) in the Gamohaan formation support generally anoxic conditions. Similarily, Kamber and Webb (2001) reported the absence of Ce anomalies in the Gamohaan stromatolites. Voegelin et al. (2010) measured the δ^{98}Mo of some Gamohaan carbonates and found

indications of a temporary oxic episode between two generally anoxic periods during Gamohaan deposition (Figure 5.2).

4.3. 2.8 Ga stromatolites, Steep Rock, Canada

Contrary to the case of the 2.52 Ga Gamohaan stromatolites, the 2.8 Ga Steep rock samples have a significantly heavier Mo isotopic composition (Figure 5.2). The difference between the Mo signature of the 2.8 Ga stromatolites and the Mo signature of the crust implies significant fractionation of molybdenum in the form of molybdate, a clear indicator of the presence of oxygen in the environment. Different publications have suggested possible whiffs of oxygen before the GOE at 2.5Ga (Anbar et al., 2007; Lyons et al., 2014), and this 2.8 Ga environment could be one of them.

4.4. 2.96 Ga stromatolites, Red Lake, Canada

Although all of the 2.96 Ga Red Lake stromatolite samples recorded fractionation of molybdenum, these sample have the largest range of Mo isotopic compositions, spanning positive to negative (from -0.57‰ to 1.05‰; Figure 5.2). The fact that there is fractionation (positive or negative) indicates the presence of free oxygen at some point in the environment. Moreover, sample P-33 shows a light value close to those of modern Mn-crusts. Such a light isotopic composition is best explained by the presence of manganese oxides in the environment, perhaps in the stromatolites themselves. Planavsky et al. (2014b) observed a similar, isotopically light signature of oxygen signature in 2.95 Ga BIF from the Pongola formation, also part of the South Africa craton (Figure 5.2). The isotopic composition of the 2.96 Ga carbonates in this study and the 2.96 Ga BIF studied by (Planavsky et al. (2014b) express the entire range of Mo isotopic signatures expected for an oxygenated environment. The BIF samples represent the lightest end-member Mo sink, while the carbonates appear to be capturing the Mo isotopic signature of residual seawater.

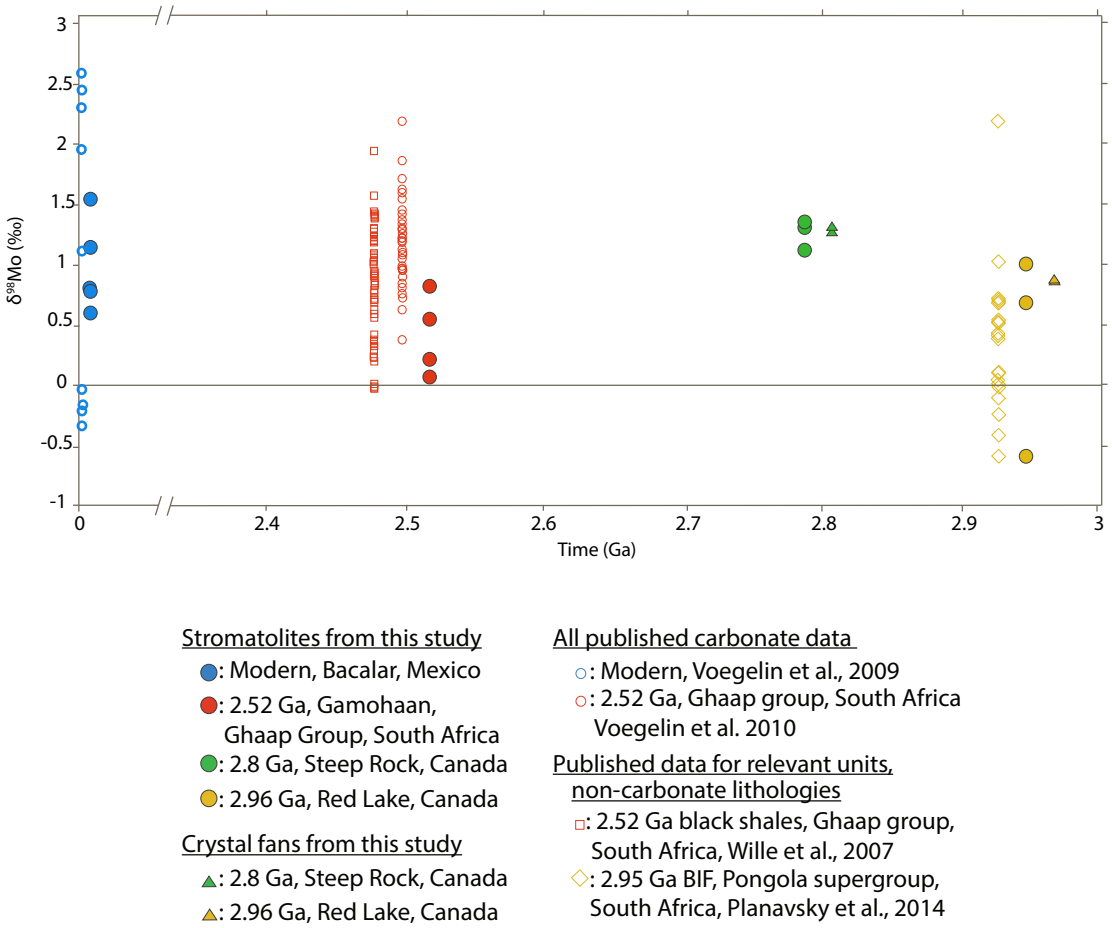

Figure 5.2: Selected Mo isotopic data throughout geological time. Mo isotopic compositions of the different types of rocks are from this study and as well as others (see legend). These results suggest a new emerging picture of redox evolution though geological time, with consistent Mo isotope evidence for at least transient oxygen in the environment at 2.96 Ga and 2.8 Ga. For comparison, data for modern carbonates and seawater are shown to present to represent the modern oxygenated environment.

4.5. Evidence for oxygen and oxygenic photosynthesis before the GOE

After the rejection of biomarkers and stromatolite morphologies as proxies for the Precambrian emergence of oxygenic photosynthesis (e.g., Rasmussen et al., 2008), elemental and isotopic proxies have become the most promising tools for constraining the beginning of the oxygenic photosynthesis on Earth.

Planavsky et al. (2014b) found evidence for this type of photosynthesis at 2.95 Ga using the light Mo isotopic composition of Mn-rich BIF. My data provide compelling evidence, using a different lithology and isotope signal (heavy vs. light), that oxygenic photosynthesis developed by 2.96 Ga. It would be interesting to investigate older stromatolites to try to find the limit between the period characterized by only anoxygenic photosynthesis (little or no Mo isotope fractionation

expected), and the beginning of oxygenic photosynthesis. It is important to note that anoxygenic photosynthesis has continued to exist throughout geological time, and is still important in selected environments (e.g., the Black Sea, certain hot springs; Repeta et al., 1989; Kulp et al., 2008). It might be tempting to use the more crustal Mo isotopic signature of stromatolites grown in anoxia environments, such as the 2.52 Ga stromatolites analysed in this study, to argue for the ancient occurrence of anoxygenic photosynthesis. However, I consider this unlikely for the 2.52 Ga stromatolites; rather, it appears that the kind of photosynthesis used by bacteria to build these stromatolites cannot be clearly defined using Mo isotopic data alone. Further analyses of iron (and perhaps sulphur) isotopes might help resolve exact photosynthetic pathways that built ancient stromatolites, and will begin soon on the same samples analyzed in this study.

While not discussed above, preliminary Mo isotopic measurements were made on crystal fans from the 2.8 Ga (Steep Rock) and 2.96 Ga (Red Lake) deposits. Contrary to the stromatolites, they originally consisted of aragonite crystals formed in shallow water without biological intervention (Pruss et al., 2008). Their Mo isotopic compositions are similar to their co-eval stromatolites (Figure 5.2), suggesting that stromatolites don't record any Mo isotope "vital effects". Other abiotic carbonate sediments (already in hand) will be explored by Mo isotopic analyses to understand the relation between molybdenum isotopic signatures and carbonate precipitation in the Archean.

Finally, multiples studies have shown evidence for "whiffs" of oxygen before the GOE (Anbar et al., 2007, Crowe et al., 2013; Planavsky et al., 2014b). This MSc project provides evidence for oxygenated periods at 2.96 Ga and 2.8 Ga (Ontario, Canada), consistent with Mo isotope evidence for oxygen by 2.95 Ga in the Pongola supergroup, South Africa (Planavsky et al., 2014b). This discovery could be taken to reflect either local and transient oases of oxygen, or alternatively, a period of mild constant oxygenation on Earth before the GOE. To better distinguish these scenarios, more molybdenum isotopic measurements and redox proxy analyses will need to be performed on Archean sediments that appear to be highly sensitive recorders of Earth's oxygenation (stromatolites, BIF).

Conclusion

Multiple studies have demonstrated the promise of sedimentary molybdenum concentrations and isotopic compositions as a sensitive redox proxy for determining paleo-oxygen levels. Modern stromatolites examined in this study appear to record Mo isotopic compositions that reflect the the water from which they grew. Preliminary Mo isotopic measurements on seawater carbonates (Voegelin et al., 2009) have demonstrated the same connection between Mo isotopic signatures of sedimentary carbonates and seawater. Thus, the Mo isotopic composition of carbonates appears to be an excellent proxy for the reconstruction of the past seawater Mo isotopic signatures, and consequently, redox in ancient marine environment. Moreover, contrary to the light isotope sink represented by Mn-crusts and BIF, carbonates record the residual heavy Mo isotope composition of seawater. The high abundance of carbonate on Earth and their independence of partial absorption of Mo make them an excellent tool for studying the Archean redox environment and for understanding the progressive oxygenation of Earth's surface environment.

This study strongly suggests that oxygenic photosynthesis could have existed since 2.96 Ga. The apparent similarity between co-eval stromatolites and crystal fans indicates minimal biological influence on Mo isotopic signatures during stromatolitic carbonate precipitation.

Various studies have suggested whiffs of oxygen at different times before the GOE, most notably in the 2.5 Ga Hamersley basin, Australia (Anbar et al., 2007), and in the 2.95 Ga Pongola formation (South Africa; Crowe et al., 2013; Planavsky et al., 2014b). In this study, 2.8 Ga and 2.96 Ga stromatolites from Canada appear to also indicate oxygen in the environment around this time. This could also be interpreted as representing pre-GOE oxygen oases, or alternatively, a long-lived period of mild oxygenation on the early Earth. Distinguishing these possibilities will require further investigation.

Bibliography

Anbar, A.D., Duan, Y., Lyons, T.W., Arnold, G.L., Kendall, B., Creaser, R.A., Kaufman, A.J., Gordon, G.W., Scott, C., Garvin, J., Buick, R., 2007. A Whiff of Oxygen Before the Great Oxidation Event? Science 317, 1903–1906. doi:10.1126/science.1140325

Archer, C., Vance, D., 2008. The isotopic signature of the global riverine molybdenum flux and anoxia in the ancient oceans. Nature Geoscience 1, 597–600. doi:10.1038/ngeo282

Arnold, G.L., Anbar, A.D., Barling, J., Lyons, T.W., 2004. Molybdenum Isotope Evidence for Widespread Anoxia in Mid-Proterozoic Oceans. Science 304, 87–90. doi:10.1126/science.1091785

Asael, D., Tissot, F.L.H., Reinhard, C.T., Rouxel, O., Dauphas, N., Lyons, T.W., Ponzevera, E., Liorzou, C., Chéron, S., 2013. Coupled molybdenum, iron and uranium stable isotopes as oceanic paleoredox proxies during the Paleoproterozoic Shunga Event. Chemical Geology 362, 193–210. doi:10.1016/j.chemgeo.2013.08.003

Awramik, S.M., 1992. The oldest records of photosynthesis. Photosynthesis Research 33, 75–89. doi:10.1007/bf00039172

Barling, J., Anbar, A.D., 2004. Molybdenum isotope fractionation during adsorption by manganese oxides. Earth and Planetary Science Letters 217, 315–329. doi:10.1016/S0012-821X(03)00608-3

Barling, J., Arnold, G.L., Anbar, A.D., 2001. Natural mass-dependent variations in the isotopic composition of molybdenum. Earth and Planetary Science Letters 193, 447–457. doi:10.1016/s0012-821x(01)00514-3

Bekker, A., Holland, H.D., Wang, P.L., Rumble, D., Stein, H.J., Hannah, J.L., Coetzee, L.L., Beukes, N.J., 2004. Dating the rise of atmospheric oxygen. Nature 427, 117–120. doi:10.1038/nature02260

Buick, R., 2008. When did oxygenic photosynthesis evolve? Philosophical Transactions of the Royal Society B: Biological Sciences 363, 2731–2743. doi:10.1098/rstb.2008.0041

Buick, R., 2008. When did oxygenic photosynthesis evolve? Philosophical Transactions of the Royal Society B: Biological Sciences 363, 2731–2743. doi:10.1098/rstb.2008.0041

Chafetz, H.S., Utech, N.M., Fitzmaurice, S.P., 1991. Differences in the 18O and 13C signatures of seasonal laminae comprising travertine stromatolites. SEPM Journal of Sedimentary Research Vol. 61. doi:10.1306/d426782a-2b26-11d7-8648000102c1865d

Collier, R.W., 1985. Molybdenum in the Northeast Pacific Ocean. Limnology and Oceanography 30, 1351–1354. doi:10.4319/lo.1985.30.6.1351

Crowe, S.A., Døssing, L.N., Beukes, N.J., Bau, M., Kruger, S.J., Frei, R., Canfield, D.E., 2013. Atmospheric oxygenation three billion years ago. Nature 501, 535–538. doi:10.1038/nature12426

DesMarais, D.J., 2000. When Did Photosynthesis Emerge on Earth? Science 289, 1703–1705.

Emerson, S.R., Huested, S.S., 1991. Ocean anoxia and the concentrations of molybdenum and vanadium in seawater. Marine Chemistry 34, 177–196. doi:10.1016/0304-4203(91)90002-e

Farquhar, J., Bao, H., Thiemens, M., 2000. Atmospheric Influence of Earth's Earliest Sulfur Cycle. Science 289, 756–758. doi:10.1126/science.289.5480.756

Gischler, E., Gibson, M.A., Oschmann, W., 2008. Giant Holocene Freshwater Microbialites, Laguna Bacalar, Quintana Roo, Mexico. Sedimentology 55, 1293–1309. doi:10.1111/j.1365-3091.2007.00946.x

Goldberg, E.D., 1954. Marine Geochemistry 1. Chemical Scavengers of the Sea. The Journal of Geology 62, 249–265.

Goldberg, T., Gordon, G., Izon, G., Archer, C., Pearce, C.R., McManus, J., Anbar, A.D., Rehkämper, M., 2013. Resolution of inter-laboratory discrepancies in Mo isotope data: an intercalibration. Journal of Analytical Atomic Spectrometry 28, 724–12. doi:10.1039/c3ja30375f

Greber, N.D., Siebert, C., Nägler, T.F., Pettke, T., 2012. δ98/95Mo values and Molybdenum Concentration Data for NIST SRM 610, 612 and 3134: Towards a Common Protocol for Reporting Mo Data. Geostandards and Geoanalytical Research 36, 291–300. doi:10.1111/j.1751-908X.2012.00160.x

Halliday, A.N., Lee, D.-C., Christensen, J.N., Walder, A.J., Freedman, P.A., Jones, C.E., Hall, C.M., Yi, W., Teagle, D., 1995. Recent developments in inductively coupled plasma magnetic sector multiple collector mass spectrometry. International Journal of Mass Spectrometry and Ion Processes 146-147, 21–33. doi:10.1016/0168-1176(95)04200-5

Heising, S., Richter, L., Ludwig, W., Schink, B., 1999. Chlorobium ferrooxidans sp. nov., a phototrophic green sulfur bacterium that oxidizes ferrous iron in coculture with a “Geospirillum” sp. strain. Archives of Microbiology 172, 116–124. doi:10.1007/s002030050748

Helz, G.R., Miller, C.V., Charnock, J.M., Mosselmans, J.F.W., Pattrick, R.A.D., Garner, C.D., Vaughan, D.J., 1996. Mechanism of molybdenum removal from the sea and its concentration in black shales: EXAFS evidence. Geochimica et Cosmochimica Acta 60, 3631–3642. doi:10.1016/0016-7037(96)00195-0

Holland, H.D., 2006. The oxygenation of the atmosphere and oceans. Philosophical Transactions of the Royal Society B: Biological Sciences 361, 903–915. doi:10.1098/rstb.2006.1838

Kamber, B.S., Webb, G.E., 2001. The geochemistry of late Archaean microbial carbonate: implications for ocean chemistry and continental erosion history. Geochimica et Cosmochimica Acta 65, 2509–2525. doi:10.1016/s0016-7037(01)00613-5

Kelly, D.P., 1974. Growth and metabolism of the obligate phototroph Chlorobium thiosulfatophilum in the presence of added organic nutriemets. Archives of Microbiology, 100:163-178

Klein, C., 2005. Some Precambrian banded iron-formations (BIFs) from around the world: Their age, geologic setting, mineralogy, metamorphism, geochemistry, and origins. American Mineralogist 90, 1473–1499. doi:10.2138/am.2005.1871

Konhauser, K.O., 2007. Introduction to Geomicrobiology. Blackwell Publishing

Konhauser, K.O., Hamade, T., Raiswell, R., Morris, R.C., Ferris, F.G., Southam, G., Canfield, D.E., 2002. Could bacteria have formed the Precambrian banded iron formations? Geology 30, 1079. doi:10.1130/0091-7613(2002)030<1079:cbhftp>2.0.co;2

Konhauser, K.O., Phoenix, V.R., Bottrell, S.H., 2001. Microbial–silica interactions in Icelandic hot spring sinter: possible analogues for some Precambrian siliceous stromatolites. Sedimentology 48, 415–433. doi:10.1046/j.1365-3091.2001.00372.x

Krajewshi, K.P., VanCappellen, P., Trichet, J., Khun, O., Lucas, J., Martin-Algarra, A., Prevot, L., Tewari, V.C., Gaspar, L., Knight, R.I., Lamboy, M., 2014. Biological processes and apatite formation in sedimentary environments. Eclogea geology 771–818. doi:10.5169/seals-167475

Kulp, T.R., Hoeft, S.E., Asao, M., Madigan, M.T., Hollibaugh, J.T., Fisher, J.C., Stolz, J.F., Culbertson, C.W., Miller, L.G., Oremland, R.S., 2008. Arsenic(III) Fuels Anoxygenic Photosynthesis in Hot Spring Biofilms from Mono Lake, California. Science 321, 967–970. doi:10.1126/science.1160799

LaBuhn, S., Burrows, C., Groff, C., Neureuther, N., Schaal, S., Volk, J., Cupul, A.F., Dominguez, A.B.M., Poot, M.M., 2012. Chemistry and Preliminary Coliform Microbial Communities in Laguna Bacalar, Yucatan Peninsula, Mexico. 1–17.

Lalonde, S.V., Konhauser, K.O., 2015. Benthic perspective on Earth's oldest evidence for oxygenic photosynthesis. Proceedings of the National Academy of Sciences 112, 995–1000. doi:10.1073/pnas.1415718112

Lyons, T.W., Reinhard, C.T., Planavsky, N.J., 2014. The rise of oxygen in Earth's early ocean and atmosphere. Nature 506, 307–315. doi:10.1038/nature13068

McManus, J., Nägler, T.F., Siebert, C., Wheat, C.G., Hammond, D.E., 2002. Oceanic molybdenum isotope fractionation: Diagenesis and hydrothermal ridge-flank alteration. Geochemistry Geophysics Geosystems 3, 1–9. doi:10.1029/2002GC000356

Mendel, R.R., 2005. Molybdenum: biological activity and metabolism. The Royal Society of Chemistry . 3404–6. doi:10.1039/b505527j

Mojzsis, S.J., Arrhenius, G., McKeegan, K.D., Harrison, T.M., Nutman, A.P., Friend, C.R.L., 1996. Evidence for lfe on Earth before 3,800 million years ago. Nature 384, 55–59.

Morford, J.L., Emerson, S., 1999. The geochemistry of redox sensitive trace metals in sediments. Geochimica et Cosmochimica Acta 63, 1735–1750. doi:10.1016/s0016-7037(99)00126-xPentecost, A. "Blue-green algae and freshwater carbonate deposits." *Proceedings of the Royal Society of London. Series B. Biological Sciences* 200.1138 (1978): 43-61.

Pavlov, A.A., Kasting, J.F., 2002. Mass-Independent Fractionation of Sulfur Isotopes in Archean Sediments: Strong Evidence for an Anoxic Archean Atmosphere. Astrobiology 2, 27–41. doi:10.1089/153110702753621321

Planavsky, N.J., Asael, D., Hofmann, A., Reinhard, C.T., Lalonde, S.V., Knudsen, A., Wang, X., Ossa Ossa, F., Pecoits, E., Smith, A.J.B., Beukes, N.J., Bekker, A., Johnson, T.M., Konhauser, K.O., Lyons, T.W., Rouxel, O.J., 2014. Evidence for oxygenic photosynthesis half a billion years before the Great Oxidation Event. Nature Geoscience 7, 283–286. doi:10.1038/ngeo2122

Pruss, S.B., Corsetti, F.A., Fischer, W.W., 2008. Seafloor-precipitated carbonate fans in the Neoproterozoic Rainstorm Member, Johnnie Formation, Death Valley Region, USA. Sedimentary Geology 207, 34–40. doi:10.1016/j.sedgeo.2008.03.005

Rasmussen, B., Buick, R., 1999. Redox state of the Archean atmosphere: Evidence from detrital heavy minerals in ca. 3250–2750 Ma sandstones from the Pilbara Craton, Australia. Geology 27, 115. doi:10.1130/0091-7613(1999)027<0115:rsotaa>2.3.co;2

Rasmussen, B., Fletcher, I.R., Brocks, J.J., Kilburn, M.R., 2008. Reassessing the first appearance of eukaryotes and cyanobacteria. Nature 455, 1101–1104. doi:10.1038/nature07381

Repeta, D.J., Simpson, D.J., Jorgensen, B.B., Jannasch, H.W., 1989. Evidence for anoxygenic photosynthesis from the distribution of bacterio-chlorophylls in the Black Sea. Nature 342, 69–72. doi:10.1038/342069a0

Rongemaille, E., Bayon, G., Pierre, C., Bollinger, C., Chu, N.C., Fouquet, Y., Riboulot, V., Voisset, M., 2011. Rare earth elements in cold seep carbonates from the Niger delta. Chemical Geology 286, 196–206. doi:10.1016/j.chemgeo.2011.05.001

Rosing, M.T., Frei, R., 2004. U-rich Archaean sea-floor sediments from Greenland – indications of >3700 Ma oxygenic photosynthesis. Earth and Planetary Science Letters 217, 237–244. doi:10.1016/S0012-821X(03)00609-5

Rosing, M.T., Frei, R., 2004. U-rich Archaean sea-floor sediments from Greenland – indications of >3700 Ma oxygenic photosynthesis. Earth and Planetary Science Letters 217, 237–244. doi:10.1016/S0012-821X(03)00609-5

Rouxel, O., Galy, A., Elderfield, H., 2006. Germanium isotopic variations in igneous rocks and marine sediments. Geochimica et Cosmochimica Acta 70, 3387–3400. doi:10.1016/j.gca.2006.04.025

Rudge, J.F., Ben C Reynolds, Bourdon, B., 2009. The double spike toolbox. Chemical Geology 265, 420–431. doi:10.1016/j.chemgeo.2009.05.010

Rudnick, R.L., Gao, S., 2003. Composition of the continental crust. Treatise on Geochemistry 1–64. doi:10.1016/b0-08-043751-6/03016-4Scott, C., Lyons, T.W., Bekker, A., Shen, Y., Poulton, S.W., Chu, X., Anbar, A.D., 2008. Tracing the stepwise oxygenation of the Proterozoic ocean. Nature 452, 456–459. doi:10.1038/nature06811

Siebert, C., Nägler, T.F., Kramers, J.D., 2001. Determination of molybdenum isotope fractionation by double-spike multicollector inductively coupled plasma mass spectrometry. Geochemistry Geophysics Geosystems 2, n/a–n/a. doi:10.1029/2000gc000124

Siebert, G.A., Hung, D.Y., Chang, P., Robert, M.S., 2003. Ion-Trapping, Microsomal Binding, and Unbound Drug Distribution in the Hepatic Retention of Basic Drugs. Journal of Pharmacology and Experimental Therapeutics 308, 228–235. doi:10.1124/jpet.103.056770

Sumner, D.Y., Bowring, S.A., 1996. U-Pb geochronologic constraints on deposition of the Campbellrand Subgroup, Transvaal Supergroup, South Africa. Precambrian Research 79, 25–35. doi:10.1016/0301-9268(95)00086-0

Sumner, D.Y., 1997. Late Archean Calcite-Microbe Interactions: Two Morphologically Distinct Microbial Communities That Affected Calcite Nucleation Differently. PALAIOS 12, 302. doi:10.2307/3515333

Thompson, J.B., Ferris, F.G., 1990. Cyanobacterial precipitation of gypsum, calcite, and magnesite from natural alkaline lake water. Geology 18, 995. doi:10.1130/0091-7613(1990)018<0995:cpogca>2.3.co;2

Thurston, P.C., Chivers, K.M., 1990. Secular variation in greenstone sequence development emphasizing Superior Province, Canada. Precambrian Research 46, 21–58. doi:10.1016/0301-9268(90)90065-x

Voegelin, A.R., Nägler, T.F., Samankassou, E., Villa, I.M., 2009. Molybdenum isotopic composition of modern and Carboniferous carbonates. Chemical Geology 265, 488–498. doi:10.1016/j.chemgeo.2009.05.015

Voegelin, A.R., Nägler, T.F., Beukes, N.J., Lacassie, J.P., 2010. Molybdenum isotopes in late Archean carbonate rocks: Implications for early Earth oxygenation. Precambrian Research 182, 70–82. doi:10.1016/j.precamres.2010.07.001

Wacey, D., Kilburn, M.R., Saunders, M., Cliff, J., Brasier, M.D., 2011. Microfossils of sulphur-metabolizing cells in 3.4-billion-year-old rocks of Western Australia. Nature Geoscience 4, 698–702. doi:10.1038/ngeo1238

Walsh, M.W., 1992. Microfossils and possible microfossils from the early archean onverwacht group, Barberton mountain land, South Africa. Precambrian Research 54, 271–293. doi:10.1016/0301-9268(92)90074-x

Wilks, M.E., Nisbet, E.G., 1985. Archaean stromatolites from the Steep Rock Group, northwestern Ontario, Canada. Can. J. Earth Sci. 22, 792–799. doi:10.1139/e85-086

Annexes

Annex 1: MC-ICP-MS, Neptune

Annex 2: Protocol of purification of molybdenum by column chromatography according to Asael et al. (2013).

Annex 3: Verification of independence between:

a: δ^{98}Mo and Double Spike/ Naturel

b : δ^{98}Mo and [Mo]

Annex 1 : MC-ICP-MS, Neptune

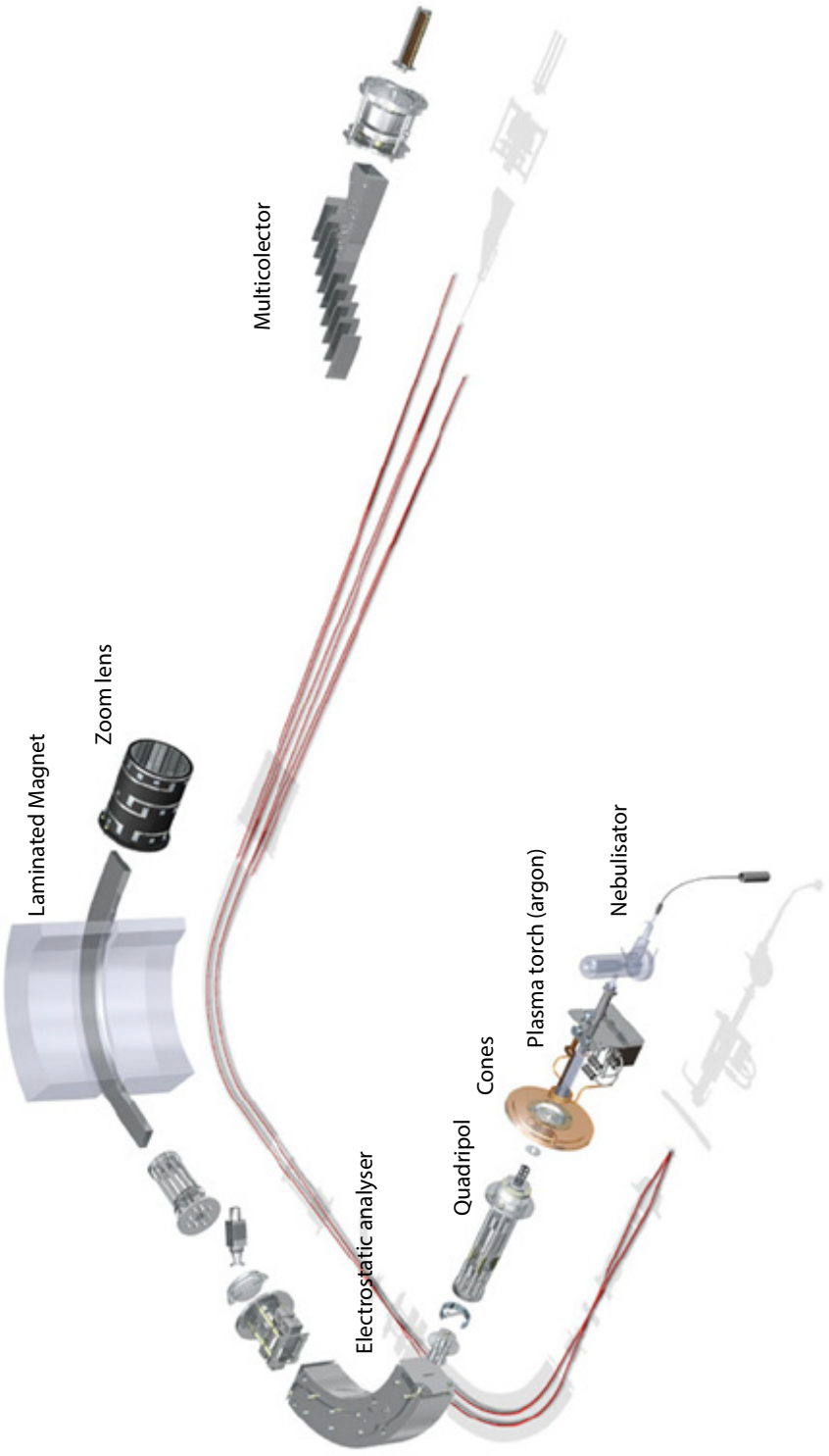

Annex 2 : Protocol of concentration of molybdenum by column chromatography according to Asael et al. (2013).

1st stage of Mo separation- anion exchange			
1ml AG 1 X8 – 200-400 mesh			
wash	**H2O**	**18.2mQ**	**2Vol.**
wash	**HNO3**	**3N**	**2Vol.**
wash	**H2O**	**18.2mQ**	**2Vol.**
conditioning	**HCl**	**6N**	**2Vol.**
sample	**HCl**	**6N**	**1ml**
matrix	**HCl**	**6N**	**2x3ml**
Mo	**HNO3**	**2N**	**3x3ml**
wash	**H2O**	**18.2mQ**	**2Vol.**
wash	**HNO3**	**3N**	**2Vol.**
wash	**H2O**	**18.2mQ**	**2Vol.**
2nd stage of Mo separation- cation exchange			
1ml AG50W X8 or 2ml if lot of iron – 200-400 mesh			
wash	**H2O**	**18.2mQ**	**2Vol.**
wash	**HCl**	**6N**	**2Vol.**
wash	**H2O**	**18.2mQ**	**2Vol.**
conditioning	**HCl**	**0.24N**	**2Vol.**
sample	**HCl**	**0.24N**	**1ml**
Mo	**HCl**	**0.24N**	**3x3ml**
Fe	**HCl**	**6N**	**2x3ml**
wash	**H2O**	**18.2mQ**	**2Vol.**
wash	**HCl**	**6N**	**2Vol.**
wash	**H2O**	**18.2mQ**	**2Vol.**

Annex 3 : Verification of independence between :

a: δ^{98}Mo and Double Spike / Naturel

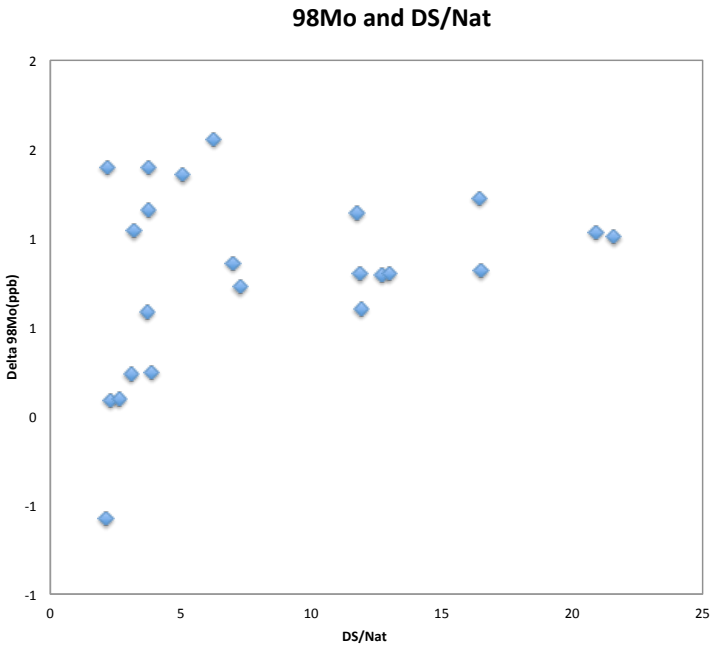

b : δ^{98}Mo and [Mo]